Tipping Point Detection on Biome States in Sub-Saharan Africa Through Time series Analysis

EUFRASIA BIANCA AMARYLLIS DIATMIKO
February, 2018

SUPERVISORS:
Dr. Ir. Thomas A. Groen
Dr. Ir. Anton Vrieling

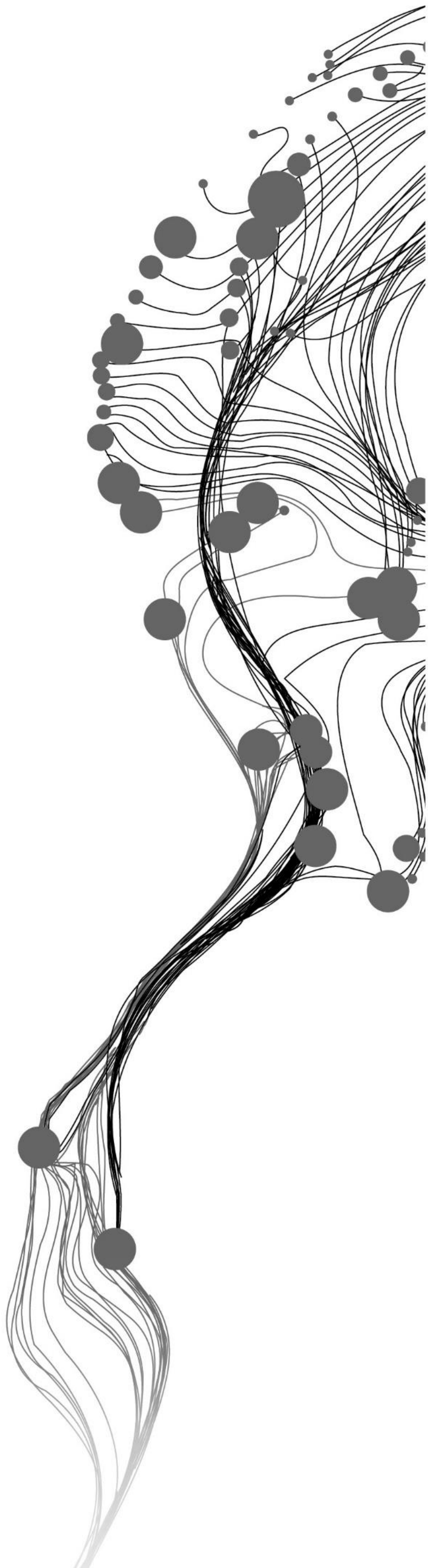

Tipping Point Detection on Biome States in Sub-Saharan Africa Through Time series Analysis

EUFRASIA BIANCA AMARYLLIS DIATMIKO
Enschede, The Netherlands, February, 2018

Thesis submitted to the Faculty of Geo-Information Science and Earth Observation of the University of Twente in partial fulfilment of the requirements for the degree of Master of Science in Geo-information Science and Earth Observation.
Specialization: Natural Resources Management

SUPERVISORS:
Dr. Ir. Thomas A. Groen
Dr. Ir. Anton Vrieling

THESIS ASSESSMENT BOARD:
Dr. Yousif A. Hussin (Chair)
Prof. Dr. Daphne van der Wal (External Examiner, ITC-WRS, University of Twente)

ABSTRACT

The increasing interest in the existence of alternative stable states grows in Africa, due to the fact that forest (characterized by high tree cover) and savanna (characterized by low tree cover) may be the alternative stable states in particular regions. Fire, as major determinant of tree cover, along with precipitation regulate the existence of alternative stable states in Africa. Analysis on bistability (where distinct biome states are found under similar environmental condition) is of importance, as potential window of opportunity for restoration efforts could be developed to reduce the risks of critical transitions to alternative stable states.

The use of remote sensing, particularly through time series analysis, could help to discover instability on biome states. This study identified the range of environmental conditions for which two distinct biome states (high and low tree cover) occur in Sub-Saharan Africa and analyzed whether statistical stability indicators (autocorrelation, standard deviation and skewness) of remotely-sensed biome state indicators (NDVI, NDWI and LST) change in a beforehand-anticipated direction towards changing environmental conditions (precipitation and fire occurrence), by using different detrending techniques in time series analysis (i.e. linear detrending, gaussian filtering and first-differencing filtering).

In this study, the frequency distributions of all the observed environmental drivers suggest that forest and savanna (high and low tree cover) might become alternative stable states at the value ranges where bistability occurs: >650 mm/year for mean annual precipitation, 0-25% for coefficient of variation of annual precipitation and zero fire count. The statistical stability indicators (autocorrelation, standard deviation and skewness) of remotely-sensed biome state indicators (NDVI, NDWI and LST) showed changes in a beforehand-anticipated direction towards changing environmental conditions. The direction of changes in statistical stability indicators was generally similar among different detrending techniques.

The performance of biome state indicators, detrending techniques and statistical stability indicators in indicating instability was assessed. NDWI was considered as the most relevant biome state indicator and autocorrelation was the most responsive statistical stability indicator in indicating instability in this study. However, all the detrending techniques applied were considered insufficient, as they could not completely cope with non-stationarity in the time series. This might be overcome by defining appropriate parameter choices (e.g. filtering bandwidth, sliding window length, degree of smoothing), to improve the performance of statistical stability indicators and remotely-sensed biome state indicators in indicating instability.

ACKNOWLEDGEMENTS

First and foremost, I gratefully acknowledge Dr. Ir. Thomas A. Groen and Dr. Ir. Anton Vrieling for their patience, continued support and constructive comments on this study. I am thankful for their guidance and I believe that I have been exceptionally fortunate to have them as my supervisors.

I am also very grateful to LPDP-Ministry of Finance, Indonesia for the scholarship granted for the entire period of my master program, that gives me a great opportunity to pursue my dreams at one of the advanced geo-information institutions in the world, ITC. Studying at ITC would never happen without LPDP's financial support.

I would like to express my deep sense of gratitude to Dr. Ir. Rolf A. de By and Lyande Eelderink, as ITC-ESRI interns committee, to give me a chance to be proposed for an internship program at the world's most powerful mapping and spatial analytics software company, ESRI. It is such an honor for me to have an exciting experience in Redlands, California.

At this moment, I would also like to thank all the NRM staff and fellow students from all over the world for sharing ideas, knowledge and experiences. Last but not least, I would like to express my heartfelt appreciation to ITC Indonesian students for wonderful time spent. Their presence makes The Netherlands, especially Enschede, feel like home and it could turn stress into happiness through togetherness. I wish all the ITC 2018's alumni the best for their future endeavours.

TABLE OF CONTENTS

LIST OF FIGURES

LIST OF TABLES

LIST OF ABBREVIATIONS

ACF(1)	:	Autocorrelation at lag-1
CHIRPS	:	Climate Hazards Group InfraRed Precipitation with Station Data
CV	:	Coefficient of Variation
LST	:	Land Surface Temperature
MODIS	:	Moderate Resolution Imaging Spectroradiometer
NDVI	:	Normalized Difference Vegetation Index
NDWI	:	Normalized Difference Water Index
OVC	:	Other Vegetation Cover
OWL	:	Other Wooded Land
SD	:	Standard Deviation
SK	:	Skewness
TC	:	Tree Cover
TCM	:	Tree Cover Mosaic
TREES	:	Tropical Forest Cover Change Assessment

GLOSSARY

Alternative stable states	:	Distinct biome states (forest and savanna) that have capability of returning to their equilibrium conditions after perturbations or do not experience unexpected large changes in their characteristics across time under a given range of environmental conditions
Autocorrelation	:	A measure expressing correlation between the elements of a series and others from the same series separated from them by a given interval (e.g. time lags of one time-step)
Biome state	:	A large ecological community type at its initial condition, formed by a set of biotic and abiotic factors (e.g. forest state and savanna state)
Biome state indicators	:	Satellite-derived products to assess temporal dynamics of biome states (NDVI, NDWI and LST in this study)
Bistability	:	The occurrence of two alternative stable states (forest and savanna) under similar environmental conditions
Critical transition	:	A qualitative change in the characteristics of a biome state when it reaches tipping point
Environmental drivers	:	Environmental factors influencing dynamics of biome states (precipitation and fire in this study)
Detrending	:	A technique of removing trend from time series, to exclude a feature considered as distortion, in analysing time series with methods that assume stationarity
Human interventions	:	Human-induced factors in determining biome distributions (agriculture and settlements in this study)
Skewness	:	A measure of the degree of asymmetry of a distribution
Standard deviation	:	A measure expressing by how much the members of a group differ from the mean value for the group
Statistical stability indicators	:	Statistical measures to detect warning signals of potential instability such as autocorrelation, standard deviation and skewness
Tipping point	:	A threshold at which a biome state switches into another state, leading to a qualitative change in the state of an ecosystem

1. INTRODUCTION

1.1. Background

The increasing interest in the existence of alternative stable states in global ecosystems suggests more observations on tree cover distributions, to explain instability on biome states as response to changing environmental conditions. This interest grows also in Africa, due to the fact that forest (characterized by high tree cover) and savanna (characterized by low tree cover) may be the alternative stable states in particular regions (Staver et al., 2011a). A resurgence of interest in alternative stable states appears to predict where distinct biome states may occur, when and why a sudden change on biome state might happen (Beisner et al., 2003).

Fire, as major determinant of tree cover (Staver et al., 2011a; Dantas et al., 2016), along with precipitation regulate the existence of alternative stable states in Africa. Precipitation has positive correlation to tree cover, while fire is negatively related (Groen et al., 2011). These relationships between tree cover and both environmental drivers (precipitation and fire occurrence) suggest the existence of alternative stable states. Due to disturbances or changes in environmental conditions, a combination of frequent fire occurrence and limited amount of precipitation in Africa could potentially lead to transitions from forest, which is referred to as biome states with high tree cover percentage, to savanna, with low tree cover (Staver et al., 2011b). These potential critical transitions on biome states could represent a threat to the maintenance of tree cover distribution in African continent.

Several cases of shifts on biome states due environmental drivers have been reported. One of them was between 1986 and 1987 during a dry season, that an area of 120,000 ha of forest and woodlands in Burkina Faso was burned and such a disaster caused a heavy loss in terms of vegetation resources (Kigomo, 2003). Another case was discovered by The Global Land Analysis and Discovery (GLAD) project conducted by University of Maryland, that hotspots consisting of huge wildfires with smaller fires nearby were detected from satellite images in Africa as the alerts of critical transitions in tree cover. These fires spread into a tract of intact forest ecosystems as of 2013 (Hansen et al., 2016). There were 91,269 hotspots recorded in 2016, while there was only a total of 331 hotspots in 2015 (Potapov et al., 2017), which was attributed to a drought event. Unpredictable precipitation dynamics have whittled away forests and would lead to more frequent fire occurrence. As a result, the probability for more outbreaks of fires to happen in the future, particularly in the Congo Basin, is getting higher (Hansen et al., 2016).

Such shifts on biome states (from high to low tree cover) were affected by changing environmental conditions on ecosystems, e.g. due to drier condition (Van Nes et al., 2014). A threshold at which a state of ecosystem switches into another state, is generally referred to as a tipping point (Scheffer et al., 2009). A gradual change under certain environmental conditions, can bring a biome state closer to a catastrophic tipping point. Tipping point acts as a threshold for a loss of resilience in the sense that even small perturbations can invoke a shift to an alternative stable state (Dakos et al., 2012). Under similar environmental conditions, two alternative stable states (forest and savanna) could possible occur, which further is referred to as bistability. When environmental condition changes to a condition at which bistability occurs, the biome state could approach tipping point, which in turn, could stimulate critical transitions to alternative stable states (Kéfi et al., 2007).

Several studies allowed to recognize the proximity of transitions to alternative stable states (Scheffer et al., 2009). There are several statistical measures, such as autocorrelation, standard deviation and skewness, as indicators of 'critical slowing down process' on biome states. Critical slowing down process occurs when a biome state is approaching a tipping point (becomes less stable), it slows down or becomes more sluggish in the response to disturbances (Lenton et al., 2012). The return time to equilibrium after a perturbation is getting longer, denoting that this disturbed biome state calls for more time to recover (Van Nes and Scheffer, 2007). Under a critical slowing down process, a biome state could switch quicker or respond more dramatically to disturbance and goes back slower to its equilibrium. These slowing down signals could be captured in increasing autocorrelation and variance, and alternatively in a rise of asymmetries in ecosystem stability, which is known as skewness. Autocorrelation, standard deviation and skewness are further referred to as 'statistical stability indicators' in this study. A marked increase in these statistical stability indicators denotes a warning signal of critical slowing down of recovery rate on biome states (Alibakhshi et al., 2017).

The use of remote sensing, particularly on time series analysis, could help to discover the risk of potential transitions from high to low tree cover percentage. The potential critical transitions could be predicted by examining ecosystem functions and properties through time series analysis. Some satellite-derived proxies are required to explain the temporal dynamics of biome state, which in this study are referred to as biome state indicators. Alibakhshi et al. (2017) suggests the importance of selecting the right biome state indicator that could explain the ecosystem instability, by exploring the use of vegetation (NDVI), water (MNDWI), and vegetation-water indices (VWR and MVWR). In that study, these MODIS satellite-derived indices were employed to evaluate the stability of a wetland ecosystem. Another study on statistical stability indicators of satellite-derived indices (biome state indicators) was carried out by Verbesselt et al. (2016), observing slowing down signals that could be reflected by temporal autocorrelation of MODIS NDVI. The value of temporal autocorrelation rises steeply with decreasing precipitation to a critical level in tropical forests, implying the fact that such forests might have higher risk to experience critical transitions when faced a drought stress.

The application of time series analysis on critical slowing down process should filter out the seasonality and other elements that could distort or obscure the important features observed in time series (Lenton et al., 2012). This could be done through detrending, to exclude any possible non-stationarities by removing the trend from time series (Dakos et al., 2012). Detrending is sometimes used as a pre-processing step before meaningful spectral results can be obtained (Wu et al., 2007), to prepare time series for analysis by methods that assume stationarity. There are several detrending techniques applied in this study, i.e. linear detrending, gaussian filtering, and first-differencing filtering. Gaussian filtering is considered as the most appropriate detrending technique to probe robust early warning signals of climate tipping points by Lenton et al. (2012), compared to linear detrending.

1.2. Research Problem

Observations on statistical stability indicators of ecosystem dynamics may allow detection of potential critical transitions. However, previous studies (e.g. research by Dakos et al. (2012) and Alibakhshi et al., (2017)) only exemplified how statistical stability indicators behaved towards critical transitions, instead of comparing the ability of each statistical stability indicator to probe robust signals of instability. Therefore, a comparative study on the performance of each statistical stability indicator would help to understand its characteristics in performing warning signals.

Until recently, the proposed methods on generating warning signals of potential instability were mostly applied on simulated ecological data (e.g. a study by Dakos et al. (2012)), rather than on time series of real ecosystems. Thus, evidences of warning signals of critical transitions in real ecosystems under certain environmental conditions are insufficient. An observation on those ecosystems is of importance as it can meaningfully contribute to a relevant implementation to reduce the risk of biome state collapses (Scheffer et al., 2009).

There were few studies that linked between two related concepts of transitions on biome states: the concept of bistability or alternative stable states and the concept of slowing down signals with the use of statistical measures (e.g. a study by Kéfi et al. (2014)). Research on these related concepts seems promising as statistical stability indicators could capture slowing down signals that can be used to illustrate the proximity of potential instability to alternative stable states.

Detrending is of great interest and importance in time series analysis (Wu et al., 2007). However, there has been only limited comparison of detrending techniques in generating warning signals of critical slowing down process from time series (Biggs et al., 2009; Drake and Griffen, 2010). A rigorous and satisfactory observation on the performance of different detrending operations is still lacking (Wu et al., 2007), especially on ecosystem instability. There are some uncertainties over the sensitivity of different detrending techniques to certain parameter choices in statistical analyses (Lenton et al., 2012). Due to a lack of observation on a proper detrending technique for slowing down signals, a comparative study on the sensitivity of detrending operations is needed.

1.3. Research Objectives

The main objective of this study is to analyze how several statistical stability indicators could suggest bistability towards changing environmental conditions in Sub-Saharan Africa through time series analysis. This main objective is divided into two specific objectives as follows:

1. to identify the range of environmental conditions for which two distinct biome states (high and low tree cover) occur in Sub-Saharan Africa;
2. to analyze whether statistical stability indicators (autocorrelation, standard deviation and skewness) of remotely-sensed biome state indicators (NDVI, NDWI and LST) change in a beforehand-anticipated direction towards changing environmental conditions (precipitation and fire occurrence), by using different detrending techniques in time series analysis (i.e. linear detrending, gaussian filtering and first-differencing filtering).

1.4. Research Questions

1. In which value ranges of environmental conditions do we find both high and low tree cover, suggesting bistability?
2. Are there changes in statistical stability indicators (autocorrelation, standard deviation and skewness) in a beforehand-anticipated direction towards changing environmental conditions (precipitation and fire) on distinct biome states (high and low tree cover)?
3. Which statistical stability indicator (autocorrelation, standard deviation and skewness) is more responsive to changing environmental conditions?
4. Which biome state indicator (NDVI, NDWI and LST) is more relevant to indicate instability in distinct biome states?
5. Which detrending technique (linear detrending, gaussian filtering and first-differencing filtering) is more appropriate to indicate instability on distinct biome states?

1.5. Research Hypotheses

To answer the objectives and research questions of this study, several hypotheses are formulated as follows:

1. The value ranges where bistability occurs vary under different observed environmental drivers. This value range could be found under intermediate level of precipitation, for example, where distinct biome states are regulated under similar environmental condition.

2. Across different locations, the values of statistical stability indicators (autocorrelation, standard deviation and skewness) on areas with high tree cover percentage, are expected to decrease with increasing precipitation, as they are assumed to stabilize at their states. On the contrary, on low tree cover percentage, the values of these statistical stability indicators would rise with increasing precipitation level. Other environmental drivers (coefficient of variation of annual precipitation and total fire count) are expected to be negatively related to tree cover distribution. Thus, they would show inverse patterns by showing increases in the statistical stability indicators despite high tree cover percentage.

3. Autocorrelation is expected to be more responsive to changing environmental conditions. More increases in autocorrelation value are expected, compared to increases in standard deviation and skewness.

4. NDVI as an index of greenness level on vegetation cover is considered to strongly represent the distribution of tree cover. Therefore, NDVI is expected to be more relevant to indicate instability on distinct biome states (high and low tree cover), compared to NDWI and LST.

5. Gaussian filtering is expected to be more appropriate to indicate instability on distinct biome states (high and low tree cover), among all the detrending techniques applied in this study.

2. STUDY AREA AND DATA

2.1. Study area

The study area covers Sub-Saharan countries in Africa, including countries in the south of the Sahara Desert and Madagascar island, shown by Figure 1. This region lies between 26^0 N to 34^0 S and 17^0 W to 51^0 E, covering a large area of 24.607.840 km^2. The climate ranges from tropical to semi-arid climate. It predominantly consists of savannas, where grasslands are dotted by scattered trees, occupying more than half of the continent's land surface (Scholes and Archer, 1997).

The climate in Africa is influenced largely by distance from the equator and altitude. The climate in the highlands is typically temperate, even though the location is nearby the equator. Precipitation is more consistent in the humid forests, despite the variability of precipitation during rainy and dry seasons (Malhi et al., 2013). Tropical climate is found in Central and Western Africa, while the semi-arid climate regulates the Sahel belt, including the countries in the south of Sahara such as Mauritania, Mali, Niger, Chad and Sudan.

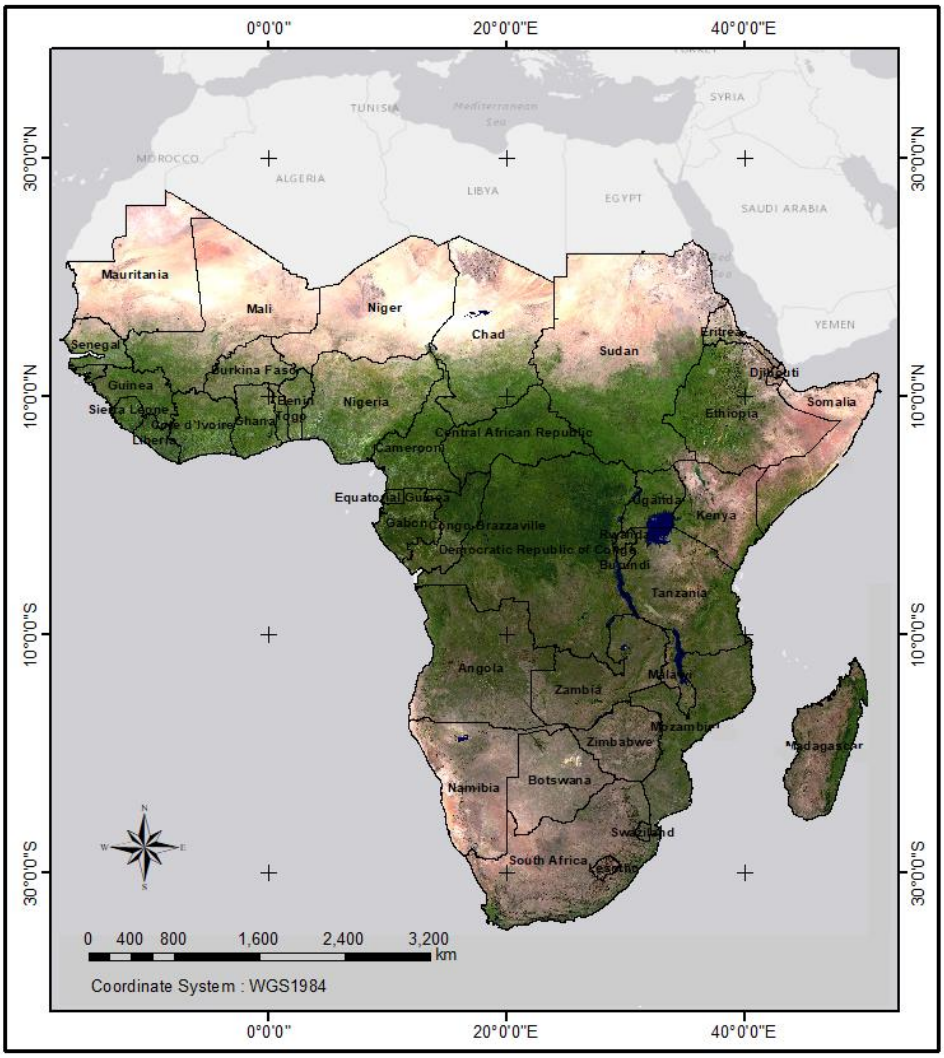

Figure 2.1. Map of study area in Sub-Saharan

Sub-Saharan Africa is covered by savanna, desert, grassland and forest. A savanna is a tropical ecosystem with woody plants (trees and shrubs) and grass, typically characterized by a broad grassland with sparse trees and herds of grazing animals such as zebra and antelope. In some cases, tree cover is found to be more than half of the area of savanna ecosystem (Scholes and Archer, 1997). The Sahel belt (shown by Figure 2.2. in yellow, in the south of the desert) is a mixed zone between semi-arid short grassland and tropical savanna, dominated by steppe vegetation that spreads across the continent from the western to the eastern region.

Forest ecosystems in Sub-Saharan Africa include tropical rainforests with a total area estimation of almost 2,000,000 km², characterized by thick, high-branched forests, surrounded by a pattern of savanna woodlands along rivers and groves of dwarf trees on mist-wrapped hills (Malhi et al., 2013). The proportion of the forest size consists of 89.3% of Central African forest, 6.0% of West African, 2.2% of forest ecosystem in Madagascar and 2.4% in Eastern Africa (Malhi et al., 2013).

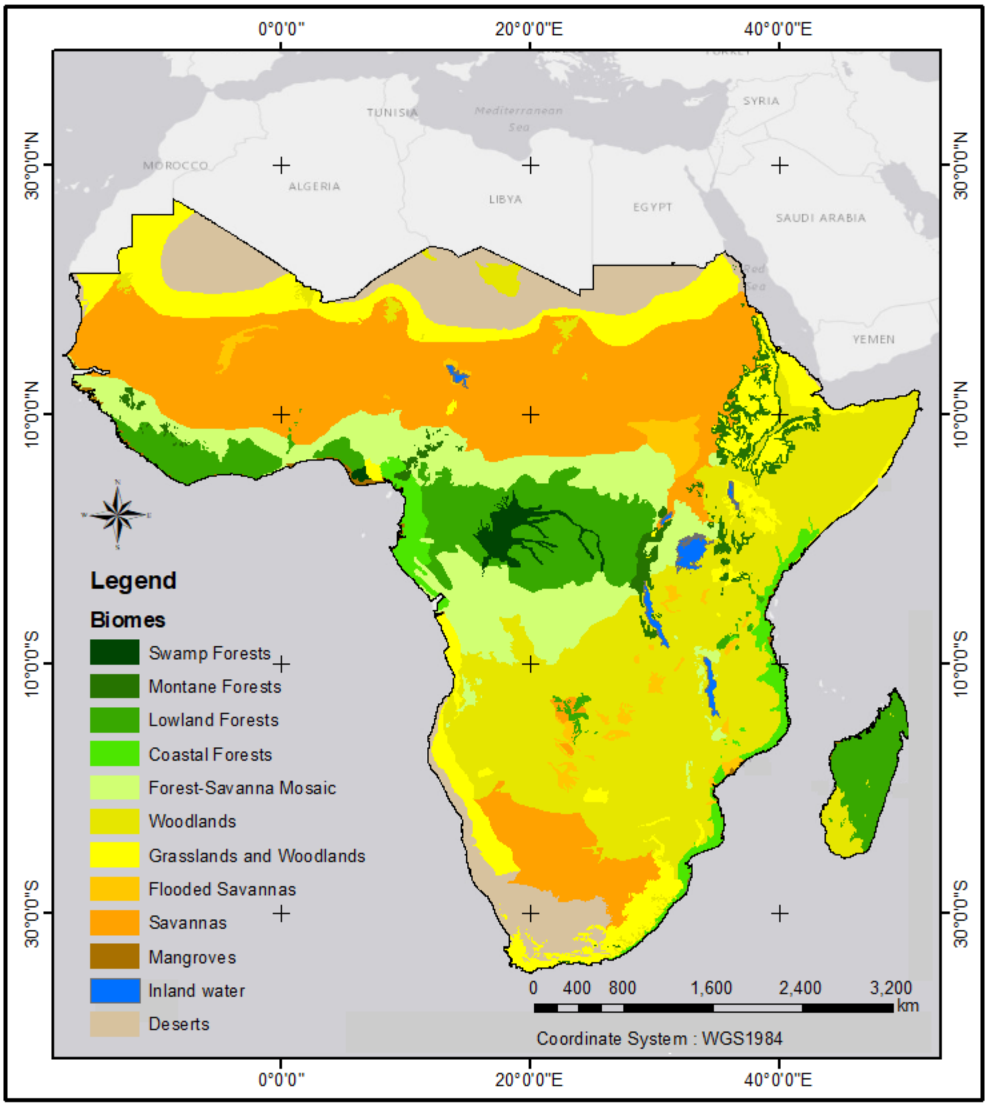

Figure 2.2. Biome distribution in Sub-Saharan Africa (modified from Olson et al., 2001)

Tropical rainforests in Sub Saharan Africa are along the southern coasts of West Africa (lowland forests) and the central mountains to the Guineo-Congolian region, stretching across Central Africa (montane forests and swamp forests in the centre), shown by Figure 2.2. The majority of the forest belongs to Democratic Republic of Congo (DRC). This accounts for 53.6% of Africa's rainforest ecosystem, followed by Gabon (11.2%), the Republic of Congo (10.4%) and Cameroon (10.0%), while the remaining countries account for 14.8% of total rainforest area (Malhi et al., 2013). Forest ecosystems are surrounded by forest-savanna mosaic (Figure 2.2.), which is found as a transitional zone between the tropical savanna in the Sahel belt and tropical forest in Central Africa.

The predominance of savanna in Sub-Saharan Africa, which is characterized by sparse trees in grasslands, has been utilized for agriculture in some parts. Annual cultivation or permanent crops occupied 1,730,000 km^2 area of the total size of Sub-Saharan Africa. Agro-pastoral sorghum farming system lies along savanna ecosystems in the Sahel belt, shown by Figure 2.2., followed by cereal fields in the south. The woodlands are also occupied by maize mixed farming system in the centre, while grasslands and savanna in Namibia and South Africa are dominated by large commercial and small-holder agricultural activities.

2.2. Data

2.2.1. Tree cover of biome state distribution

To calculate tree cover percentage, this study used tree cover data from the Joint Research Centre (JRC) of the European Commission (http://forobs.jrc.ec.europa.eu/trees3) called TREES (Tropical Forest Cover Change Assessment) product. This product is an output of Forest Observations (FOROBS) project which aims to develop methods for monitoring forest resources and carbon emissions by using multi-temporal Landsat satellite images (TM and ETM+ sensors). The project was conducted for assessing tree cover changes on tropical forests from 1990 to 2000 and 2000 to 2010. Tree cover data used in this study were between 2000 and 2010.

TREES data comprise 2,006 sample units distributed across Sub-Saharan Africa in a systematic sampling approach between 26^0 N and 34^0 S, covering tropical and subtropical regions (Figure 2.2). The size of the sample unit is 10 x 10 km each, located at every one degree latitudinal and longitudinal confluence point. The data are in Universal Transverse Mercator (UTM) projection and with minimum mapping unit of 5 ha (Achard et al., 2014). However, there were several missing sample units mostly located in cloudy areas over the coastal regions of Gabon, Congo and Cameroon.

TREES data are the classified Landsat imagery with spatial resolution of 30 m for the classification on land use and land cover of each sample unit (10 x 10 km). Those Landsat images were segmented by using eCognition software, followed by digital classification and object-based change detection (European Commission, 2015). The process of quality control required the use of image analysis tools for visual assessment of all sample units and validation of the classification and change detection. This validation process involved forestry experts from tropical countries.

The use of TREES data in this study was motivated by a study (Achard et al., 2014) that tree cover classification on TREES data underwent robust control chain. This was also supported by Gross et al. (2017), through a comparison of tree cover classification among three different tree cover data: TREES data, MODIS VCF (Vegetation Continuous Field) and GFC (Global Forest Change Map). The results of tree cover assessment showed high agreement between TREES data and cross-reference: 94% on forest labels and 90.2% on forest change labels, between sample units and a systematic reinterpretation by independent experts on sample polygons. This assessment involved visual checking on each sample unit by forestry experts through a manual correction of the mislabelled polygons after the automatic segmentation and labelling process in TREES data. Landsat high-resolution images were used as reference data for cross comparison of tree cover classification.

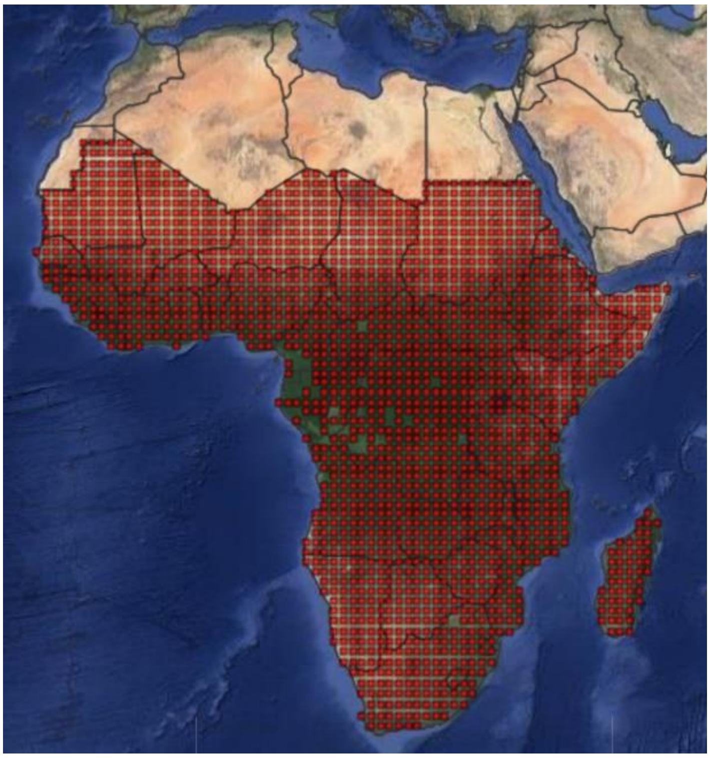

Figure 2.3. Sampling Design of TREES Product (taken from http://forobs.jrc.ec.europa.eu/trees3)

Land cover classes on TREES data are classified into tree cover (TC), tree cover mosaic (TCM), other wooded land (OWL), water (W) and other land cover (OLC) including bare and artificial, other vegetation cover (agriculture and grasslands), cloud and shadow, burned area, no data and unclassified. The classification of these five land cover classes is based on tree cover density on the polygon fraction covered by trees. Tree cover class (TC) accounts for 70-100% of woody vegetation density with tree height of >5 meters, whereas tree cover mosaic (TCM) has 30-70% of density with the same tree height criterion (Gross et al., 2017). All other woody areas with tree height of <5 meters including shrubs and forest regrowth are classified as other wooded land, with density of <30%. Tree classes (TC and TCM) include natural forests, mature forest plantations and tree cover outside forest. Whilst, other wooded land (OWL) class covers shrubs, regrowth, forest plantations in initial growth stages and oil plantations (Stibig et al., 2014).

2.2.2. Environmental Drivers

The occurrence of two distinct biome states (high and low tree cover) were observed under precipitation and fire occurrence, as environmental drivers of tree cover in Africa (Staver et al., 2011a; Hirota et al., 2012; Dantas et al., 2016). Data used on environmental drivers were in the same period as tree cover data (2000-2010). The characteristics of the data on tree cover and environmental drivers are shown in table 2.1.

Table 2.1. Data Characteristics on Tree Cover and Environmental Drivers

Information	Tree Cover	Environmental Drivers	
		Precipitation	Fire occurrence
Name of Product	TREES	CHIRPS	MCD45A1 (Burned Area)
Projection	UTM	WGS 84/Lat-long	Sinusoidal
Version	TREES-3	CHIRPS 2.0	V051
Spatial Resolution	10 km	0.05°	500 m
Temporal Resolution	10 years	5-day	monthly

2.2.2.1. Precipitation

The datasets used for precipitation were from CHIRPS, which stands for Climate Hazards Group InfraRed Precipitation with Station Data (http://chg.geog.ucsb.edu/data/chirps). Precipitation data by CHIRPS have been collected since 1981 to near-present, incorporating 0.05° spatial resolution satellite imagery with in-situ station data. It produced gridded precipitation time series for trend analysis and seasonal drought monitoring. CHIRPS data were developed to deliver reliable, up to date, and more complete datasets for early warning signals (such as trend analysis and seasonal drought monitoring), because estimates derived from satellite data often underestimate the intensity of extreme precipitations events. CHIRPS could remove systematic bias while precipitation grids in the past suffered in rural regions where there are less rain gauge stations.

CHIRPS data were used in this study as it performs better in estimating precipitation compared to other precipitation data such as TAMSAT (Tropical Application of Meteorology using Satellite and other data) and ARC (Africa Rainfall Climatology) in East Africa. Long term validation has been done by Dinku (2014) in Ethiopia, East Africa, using different precipitation infrared products against in-situ measurements, resulting in better correlation in CHIRPS. Another validation on precipitation data was done by Funk et al. (2015) using GPCC (Global Precipitation Climatological Centre) stations as references, showing less bias with average of 0.22 on CHIRPS, compared to other satellite products such as TRMM (Tropical Rainfall Measuring Mission) and CFS (Coupled Forecast System) over African continent in the wettest three months of the years during 2000-2010.

2.2.2.2. Fire Occurrence

Data on fire occurrence were derived from the MODIS (Moderate Resolution Imaging Spectroradiometer) burned area product. Burned areas and data quality information per-pixel basis on monthly MCD45A1 data were collected by both MODIS Terra and Aqua satellites at spatial resolution of 500 meters (https://lpdaac.usgs.gov). MODIS data were also used to examine the temporal dynamics of biome state indicators in this study, explained in Section 2.2.3.

MCD45A1 product provides an estimate of fire occurrence per pixel, derived from daily surface reflectance inputs, using a bidirectional reflectance distribution function (BRDF) model-based for change detection (Staver et al., 2011a). The algorithm involves a statistical measure to identify the change probability from a previously observed state. These cloud-screened datasets are atmospherically and geometrically corrected. An image-band of the direction of fire was used to calculate total fire count in this study.

This study used MCD45A1 product as motivated by a validation work on fire datasets across African biome states with a result of high accuracy in MCD45A1 in open systems, done by Tsela et al. (2014). This validation work reported that MCD45A1 appeared more reliable than other MODIS burned area products, e.g. MCD64A1, in detecting burned area fractions on less than 50% of a MODIS pixel. The product performed higher detection probabilities across all burned area proportions in South Africa, compared to MCD64A1.

2.2.3. Biome State Indicators

To generate warning signals of instability and relate it to the occurrence of distinct biome states (bistability), this study examines temporal dynamics of biome states from satellite-derived products, referred to as biome state indicators in this study. The observation period on biome state indicators was 17 years (January 2000 - December 2016), longer than the period on tree cover data and environmental drivers. The data duration was set longer as longer time series are expected to better support the analysis on statistical stability indicators (autocorrelation, standard deviation and skewness). The observed biome state indicators are NDWI (Normalized Difference Water Index), NDVI (Normalized Difference Vegetation Index) and LST (Land Surface Temperature).

Compared to other sensors such as AVHRR and Landsat, MODIS (Table 2.2) is considered to have appropriate temporal and spatial resolution for this study. MODIS has a relatively long duration (since 2000) to support long time series analysis. AVHRR has the longest time duration among these sensors (since 1979), but the spatial resolution is too coarse, which is four or eight kilometers in Africa, while MODIS could have up to 250 meters resolution. MODIS has frequent revisit time (one to two days), while Landsat has revisit time of 16 days. The characteristics of the data on biome state indicators are shown in Table 2. MODIS data on biome state indicators used are as follows:

- Surface Reflectance (MCD43A4) for NDVI and NDWI
- Land Surface Temperature and Emissivity (MOD11A2) for LST

Table 2.2. Data Characteristics on Biome State Indicators

Information	Biome State Indicators	
	NDVI & NDWI	**LST**
Name of Product	Surface Reflectance	Land Surface Temperature and Emissivity
Code of Product	MCD43A4	MOD11A2
Level	L3	L3
Version	V006	V006
Temporal frequency	16-day	8-day
Spatial Resolution	500 m	1 km

MODIS Surface Reflectance (SR) and LST products consist of different data elements. MODIS SR product comprises surface reflectance, the day of the year for the pixel along with solar, view, and zenith angles, while MODIS LST product has day time and night time LSTs, observation times, bits of clear-sky days and nights, and emissivity estimated in band 31 and 32 from land cover types. These MODIS data provide adequate information on data quality and have been corrected for atmospheric scattering or absorption due to gases and aerosols. These data were validated to stage 2, which means that the accuracy has been assessed over a widely distributed set of locations and time periods.

3. METHODS

The workflow of this study was divided into two sections based on the objectives, shown by Figure 3.1. The first section is analysis on bistability under environmental conditions, while the second is analysis on statistical stability indicators towards changing environmental conditions. Three different software and programming tools were used in this study, i.e. ArcGIS, Google Earth Engine and R-environment. ArcGIS model builder was used to handle all TREES sampling units over Sub-Saharan Africa. Data extraction on environmental drivers and temporal dynamics of biome states indicators was done by using Google Earth Engine. R-environment was used to calculate statistical stability indicators on each sample and to process a regression analysis towards changing environmental conditions.

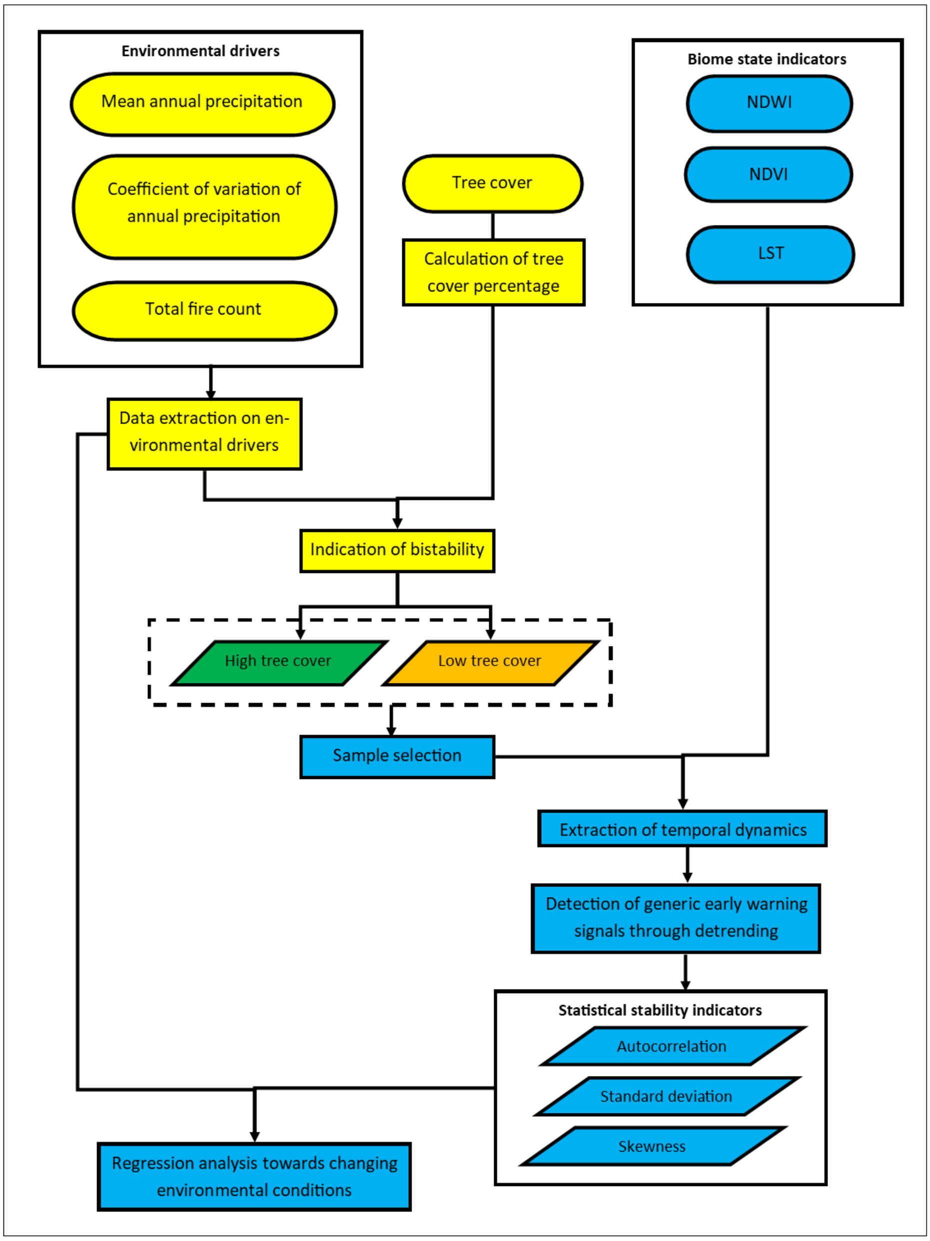

Figure 3.1. Workflow of the methodology, consisting of two main processes in this study: the first objective (yellow) and the second objective (blue)

3.1. Analysis on bistability under environmental conditions

3.1.1. Calculation of tree cover percentage

Individual sample units of TREES data over Sub-Saharan Africa (2,006 units in total with the size of 10 x 10 km) were merged into a large combined shapefile through iteration process in ArcGIS model builder. However, this iteration process could not run before the projection system of each sample unit was defined. There were 215 out of 2,006 sample units that had missing or unknown spatial reference information. If the projection system was not defined, this would have resulted in either the absence of 215 sample units on the combined shapefile or an issue of overlapping sample units after the merging process. Nevertheless, as the projection system of TREES data is in Universal Transverse Mercator (UTM) which is inherently attributed to specific zones, the projection system of these missing samples could not be generalized through an automatic process in model builder with the use of iteration function. The merging process of individual sample units was done after the projection system of each missing sample was defined in UTM zone manually.

Tree cover (TC) and tree cover mosaic (TCM) classes of TREES data in 2000 (representing data between 2000 and 2010) on the merged shapefile were selected and dissolved separately at a sample-unit basis (10 x 10 km). Before the area calculation was done on the polygons of TC and TCM on each sample unit, the projection system of the merged shapefile was converted to Albers Equal Area Conic. The shapefile was re-projected to Albers Equal Area Conic because area calculation in UTM would enlarge the size of the sample unit to exceed 10 x 10 km in some locations, particularly near the equator. In consequence, this would lead to overestimation on the calculation of tree cover percentage in those locations. Therefore, to avoid this issue, a reprojection process became essential and Albers Equal Area Conic was considered suitable for Africa, enabling an equal area calculation across the continental scale, regardless the geographical position (ESRI, 2012).

The calculation of tree cover percentage involves TC and TCM areas as these classes were considered as areas covered by trees. Areas of human interventions such as agriculture and settlements were excluded from the calculation of tree cover percentage. As grassland is classified into the same class with agriculture in Other Vegetation Cover (OVC) on TREES data, grassland was also excluded from this study. The exclusion of these areas was done because it might happen on a sample unit that a small TC or TCM area is more influenced by human interventions, instead of environmental drivers, especially for an area that is surrounded or adjacent to agriculture and settlements. Instead, tree cover percentage on each sample unit was calculated based on the size of nature, rather than the size of sample unit (10 x 10 km). TC, TCM and other wooded land (OWL) were classified into nature, aiming to exclude Other Vegetation Cover (OVC) and bare and artificial classes that consist of agriculture and settlements respectively. The polygons of TC and TCM on each sample unit were assumed to have 100% and 50% of tree cover density respectively from its total area classified (Bodart et al., 2013; Mayaux et al., 2013; Achard et al., 2014; Gross et al., 2017). Therefore, to compute tree cover percentage, the following equation was used:

$$T_{sample} = \frac{TC_{2000} + 0.5(TCM_{2000})}{N_{2000}} \; X \; 100\% \tag{1}$$

Where:
T_{sample} = tree cover percentage
TC_{2000} = area of tree cover in 2000-2010
TCM_{2000} = area of tree cover mosaic in 2000-2010
N_{2000} = area of nature, consisting of TC, TCM and other wooded land

3.1.2. Data extraction on environmental drivers

For analysis on bistability under environmental conditions, data on environmental drivers was extracted in Google Earth Engine. In accordance with the observation period of tree cover, data observed on these environmental drivers were also between 2000 and 2010. The data extraction was done on an image collection of each environmental driver (mean annual precipitation and total fire count). These image collections consist of two stacks of images (CHIRPS and MODIS MCD45A1 images). Values of coefficient of variation of annual precipitation was obtained from the extraction of standard deviation of annual precipitation in Google Earth Engine. Mean and standard deviation of annual precipitation were computed, as shown in Equations (2) and (3). The calculation result of each environmental driver that was recorded on a single-band image was clipped with tree cover extent at a sample-unit basis in Sub-Saharan Africa, consisting of TC and TCM areas. This single image was clipped by using 'reduce region' function, or in GIS is known as 'clip' feature. Rather than sample (n-1), number of items in the population (N) was used as denominator to calculate both mean and coefficient of variation of annual precipitation, as this aimed to calculate the statistics of a population, rather than of a sample of that population. The algorithms for mean, standard deviation and coefficient of variation of annual precipitation were calculated as follows:

$$\mu = \frac{1}{N}\sum_{t=1}^{N} z_{\mathrm{t}} \tag{2}$$

$$SD = \sqrt{\frac{1}{N}\sum_{t=1}^{N}(z_{\mathrm{t}} - \mu)^2} \tag{3}$$

$$\mathrm{CV} = \frac{SD}{\mu} * 100 \tag{4}$$

Where:
μ = mean annual precipitation (mm/year)
z_{t}= annual precipitation in t year (mm)
N = number of observations (year)
SD=standard deviation of annual precipitation (mm/year)
CV=coefficient of variation of annual precipitation (%)

For total fire count, values of fire direction per month within 2000-2010 from each single image of MODIS MCD45A1 were extracted on tree cover extent in Google Earth Engine. 'Direction' band on MCD45A1 image provides information on the fire direction in time in which burning was detected. The values of fire direction were coded as 1 for forward direction, 2 for backward direction, 3 for both directions and 0 for no fire. These values were subsequently converted into two classes of fire: fire (1) and no fire (0). The values of 1, 2 and 3 on fire direction were reclassified into fire, while the value of 0 on fire direction was for no-fire class. These new values (either one or zero for fire and no fire respectively) were compiled and all these fire occurrences (values) were added up to a total count for each sample unit of TREES data (10 x 10 km) with tree cover extent. The compilation and reclassification processes were done in R-environment, resulting in total fire count.

3.1.3. Indication of bistability

Condition of bistability was observed by plotting tree cover against each environmental driver, shown in grey by Figure 3.2.a. This scatter plot gives an indication of under which precipitation condition two alternative stable states could occur. Figure 3.2.b shows tipping points (T1 and T2) as thresholds of the condition of bistability, separated by grey line. Dakos et al. (2012) explained tipping points under grazing rate as environmental driver towards critical transitions on resource biomass. In this study, the concept by Dakos et al. (2012) can be adapted. With decreasing mean annual precipitation, tree cover gradually declines up to critical threshold that tree cover undergoes a critical transition through a tipping point (T1). At this point, tree cover collapses to the alternative state (low tree cover). If precipitation is restored, tree cover returns to the previous state (high tree cover) at another threshold (T2). The black lines represent equilibria, while the grey line marks the boundary between two alternative stable states. Due to disturbance under bistable condition, the grey line suggests the likelihood of transitions of biome states to high tree cover in up direction, by passing T1, and to low tree cover in down direction, through T2. The results on this observation (where bistability could happen) contributed to the analysis on the occurrence of alternative stable states under certain environmental condition. In this study, the grey area in Figure 3.2., where bistability takes place, was analyzed under mean annual precipitation, coefficient of variation of annual precipitation and total fire count.

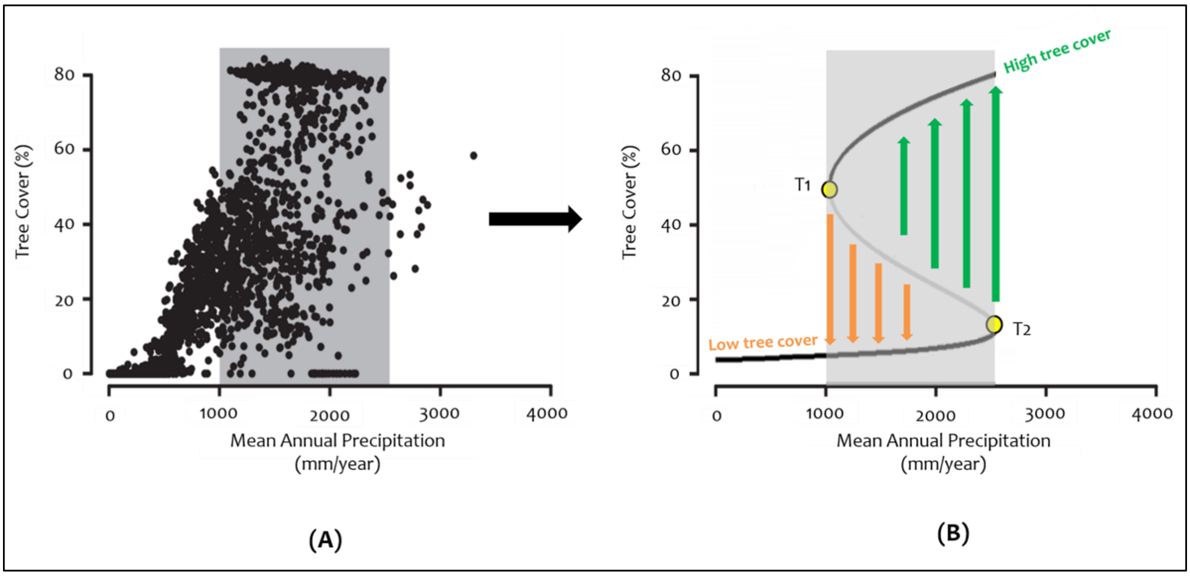

Figure 3.2. Bistable condition under mean annual precipitation, modified from Hirota et al., 2012 (A) and Kéfi et al., 2007 (B)

3.2. Analysis on statistical stability indicators on distinct biome states

3.2.1. Sample selection and extraction of temporal dynamics

Based on the results of bistability on tree cover distribution under certain environmental conditions on the first objective, 30 sample units were selected for high tree cover and 30 for low tree cover percentage. These sample units were no longer in the size of 10 x 10 km, but only with the extent of tree cover. These samples were obtained through random selection from the top 5% and bottom 5% of the total sample units. This percentage accounts for 54 sample units out of 1,086 sample units, on areas covered by trees (samples with >0% tree cover percentage). Temporal dynamics of biome state indicators (NDVI, NDWI and LST) between 2000 and 2016 were extracted for these 30 sample units on each biome state (high or low tree cover).

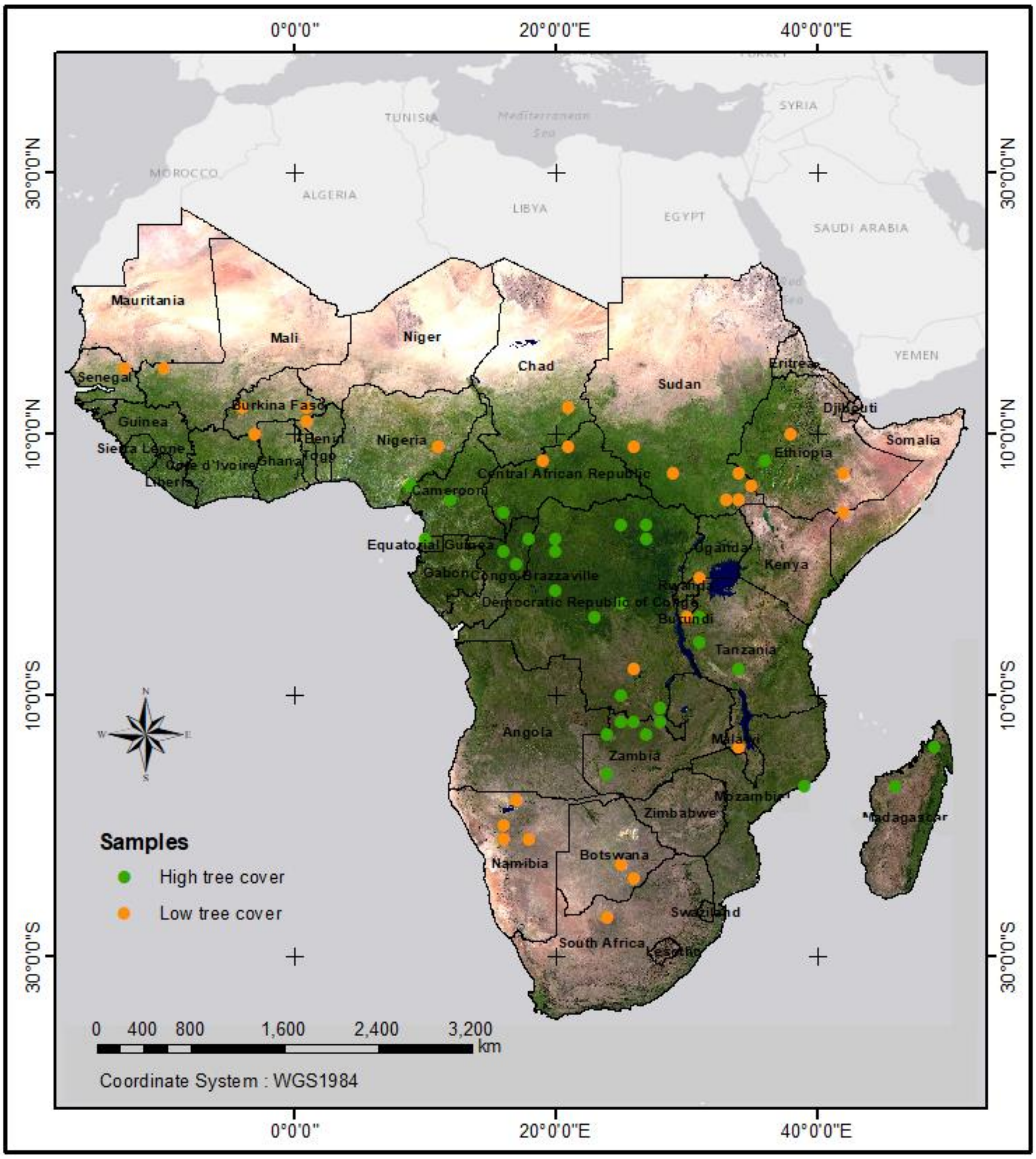

Figure 3.3. Sample distribution over Sub-Saharan Africa

A function called 'chart image series by region' in Google Earth Engine was used to extract time series data of biome state indicators on each sample unit from an image collection of environmental driver in csv format. This function in GIS is similar with 'clip' function, with areas covered by trees as a 'clip' feature. The result of the clip function on each sample unit was displayed as a chart, consisting of temporal dynamics of a biome state indicator. The data extraction could only be done in limited number of sample unit in one process in Google Earth Engine (per sample unit or up to 5 sample units). This study provides the programming scripts for extracting data on environmental drivers in Appendix 5 (a-c). The merging process of separate csv table for each sample unit was subsequently done in R-environment.

Figure 3.4. shows temporal dynamics of NDVI in 2000-2016 on two sample units (on high and low tree cover). NDVI temporal dynamics on both distinct biome states could be obviously distinguished. On high tree cover (A), NDVI values were higher and tend to persist as forest (dense vegetation) at 0.5 – 0.8, while on low tree cover (B), the values were relatively low, ranging between 0.3-0.45. Nevertheless, due to the seasonality, the values dropped considerably to between 0.25-0.5 on high tree cover and between 0.15-0.13 on low tree cover. The seasonal fluctuations were clearly captured on the charts not only in NDVI values, but also in other biome state indicators (NDWI and LST values). As this seasonality issue could affect analysis on statistical stability indicators, in the next step of this study, several techniques in time series analysis called detrending were applied to remove the seasonal or periodic components from time series.

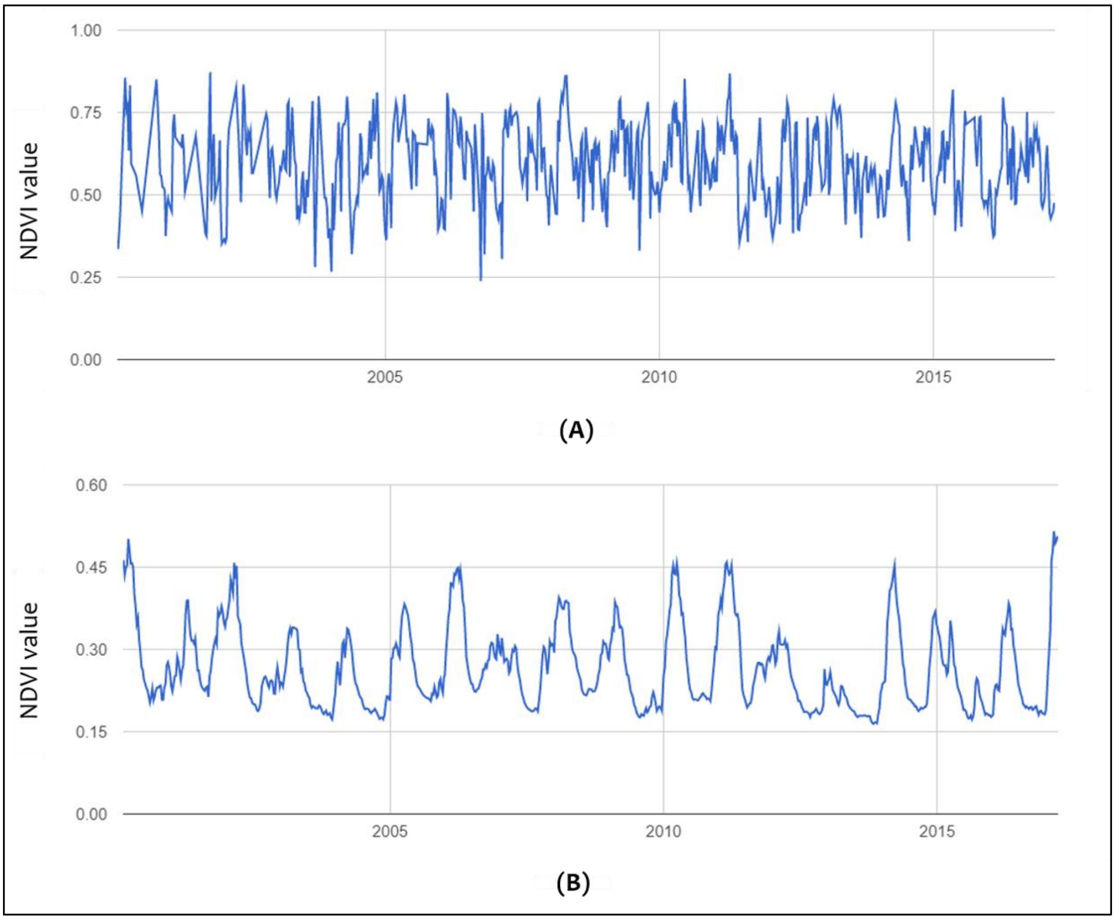

Figure 3.4. Temporal dynamics of NDVI on an area with high tree cover located at 2^0 N and 10^0 E (A) and an area with low tree cover located at 27^0 S and 24^0 E (B)

3.2.2. Detection of generic early warning signals by using detrending techniques

The merged csv table of 30 sample units on each biome state (either high or low tree cover) was the input for detection of early warning signals of instability. This detection of warning signals of instability on distinct biome states was done in R-environment with the use of 'earlywarnings' package and 'generic_ews' function (Dakos et al., 2012; Alibakhshi et al., 2017). The trends on statistical stability indicators (autocorrelation, standard deviation and skewness) were analyzed on each of those 30 sample units on each biome state, whether they have positive trends in indicating instability.

Autocorrelation is considered as the simplest statistical measurement to identify slowing down processes as warning signals of critical transitions. An increase in lag-1 autocorrelation indicates that a state becomes more similar between consecutive observations (Alibakhshi et al., 2017). It is calculated by considering a certain time lag, e.g. time lags of one time-step or lag-1 autocorrelation. In this study, time lags of one time-step was in year. Hence, the observation period of temporal dynamics of biome state indicator was moved to 2001-2017 window for analysis on autocorrelation.

The decrease in recovery rate for a state to return to the previous state also stimulates an increase in variance as well as standard deviation. Also, the distribution of the values in time series might become asymmetric due to slowing down signal, where a state may reach more extreme values close to a transition in a short time period. In consequence, this would lead to a rise in skewness. The tails of the data distribution become larger due to the increased presence of rare values in the time series (Dakos et al., 2012). Increases on the values of statistical stability indicators suggest that the ecosystems slowed down, showing as warning signals for instability, while the negative trends (decreases) suggest that the ecosystems stabilized at their states and less likely to experience critical transitions. The statistical stability indicators for detecting signals of instability were calculated as:

$$\rho 1 = \frac{E[(z_{\mathrm{t}} - \mu)(z_{\mathrm{t+1}} - \mu)]}{{\delta_{\mathrm{z}}}^{2}} \tag{5}$$

$$SD = \sqrt{\frac{1}{n-1}\sum_{t=1}^{n}(z_{\mathrm{t}} - \mu)^2} \tag{6}$$

$$SK = \frac{\frac{1}{n}\sum_{t=1}^{n}(z_{\mathrm{t}} - \mu)^3}{\sqrt{\frac{1}{n}\sum_{t=1}^{n}(z_{\mathrm{t}} - \mu)^2}} \tag{7}$$

Where:
z_{t}= variable
μ = mean
δ = variance of variable z_{t}

To take the seasonality out from the time series (as explained in section 3.2.1), detrending techniques were applied in different parameters. Detrending is a statistical operation to remove a feature thought to distort or obscure the observed feature in time series, by removing the trend (Lenton et al., 2012). Detrending is often applied as a pre-processing step to prepare time series for analysis by methods that assume stationarity.

Owing to possible non-stationarities in time series data, it is useful to remove trends before estimating statistical stability indicators to indicate the slowing down process (Lenton et al., 2012). Several different detrending methods were applied to the time series data: gaussian filtering, first-differencing, and linear detrending, to eliminate the effect of nonstationary conditions (Alibakhshi et al., 2017). Linear detrending is the simplest technique to deal with non-stationarities in mean value in time series (Held and Kleinen, 2004). This technique can work only within narrow to medium window size, as in large windows, a highly non-stationary data could introduce large bias (Lenton et al., 2012). Gaussian filtering fits a Gaussian kernel smoothing function for the time series period prior to transition (Dakos et al., 2009). The kernel function is subtracted from the record to obtain the residual data series and the choice of bandwidth for this function determines the degree of smoothing (Lenton et al., 2012). A time series that is non-stationary in mean (e.g., trend in mean) can be made stationary by taking the first difference, by applying first-differencing filtering (Larsson and Vasi, 2012). Besides the first difference of the time series, stationarity can be induced by taking the second difference, or the first difference of the first difference.

In this study, firstly, the statistical stability indicators were estimated without detrending the time series, to discover how detrending affects the results of temporal dynamics of biome state indicators, shown by the difference in the values of statistical stability indicators. Subsequently, the aforementioned detrending techniques were applied. A bandwidth of one-year period (out of 17 years) for gaussian filtering was used to filter the time series data to cope with seasonal effects on the temporal dynamics of biome state indicators. In applying linear detrending, time series were interpolated, so as to tackle the gaps in the entire time series as there were some missing values on the time series of biome state indicators. The window size was defined for the entire length of the time series (between 2000 and 2016), but since setting a 100% window size could not give any value of statistical stability indicators, the window size of 99% was applied. Warning signals of instability on distinct biome states (high and low tree cover) are shown by Figure 3.5 through increases in the values of statistical stability indicators. In this figure, temporal dynamics of NDVI (in Figure 3.4.) on both distinct biome states, were detrended by using linear detrending.

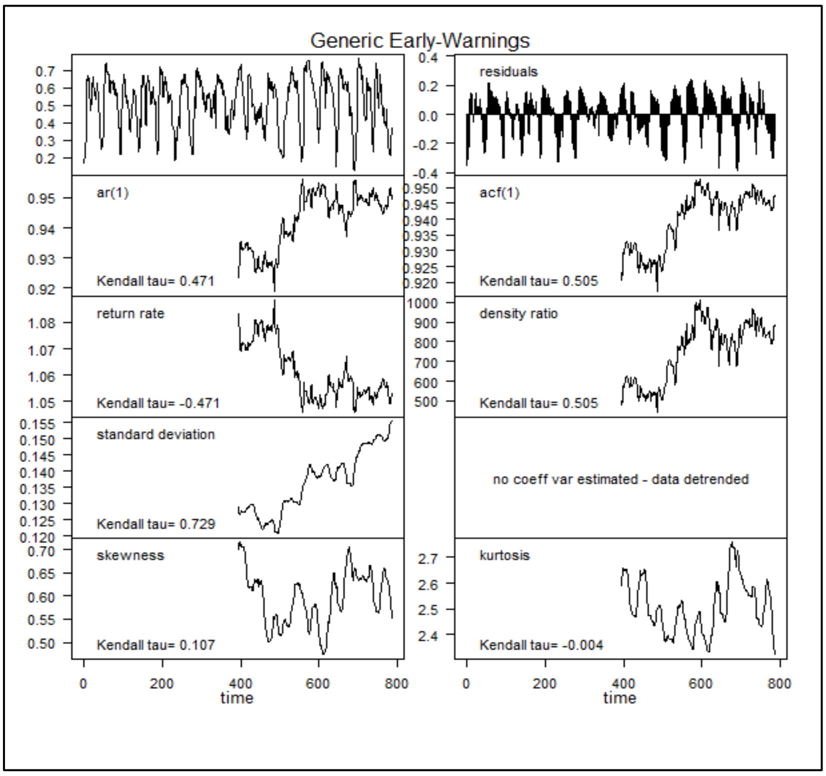

Figure 3.5. NDVI time series profile and detection of early warning signals of a sample located at 2^0 N and 10^0 E (left) and an area with low tree cover located at 27^0 S and 24^0 E (right), with the use of linear detrending method, performing increases in the values of statistical stability indicators (autocorrelation, standard deviation and skewness)

3.2.3. Regression analysis on statistical stability indicators towards changing environmental conditions

How statistical stability indicators (autocorrelation, standard deviation and skewness) vary along increasing environmental conditions (precipitation and fire occurrence) was observed through regression analysis in R-environment. This was done also to select the relevant biome state indicator in indicating instability, based on the changes in the values of statistical stability indicators. The performance of each statistical stability indicator was analyzed to discover the most responsive indicator in indicating instability.

Whether or not the changes in statistical stability indicators in a beforehand-anticipated direction could be captured, determines the analysis on the most relevant biome state indicator and the most responsive statistical stability indicator in indicating instability on distinct biome states. More corresponding values (increases on unstable states or decreases on stable states) as what were expected suggest a qualitative assessment that such biome state indicator is relevant and a statistical stability indicator is responsive in indicating instability on distinct biome states. This was also done by comparing the R^2 and p values among the biome state indicators and statistical stability indicators.

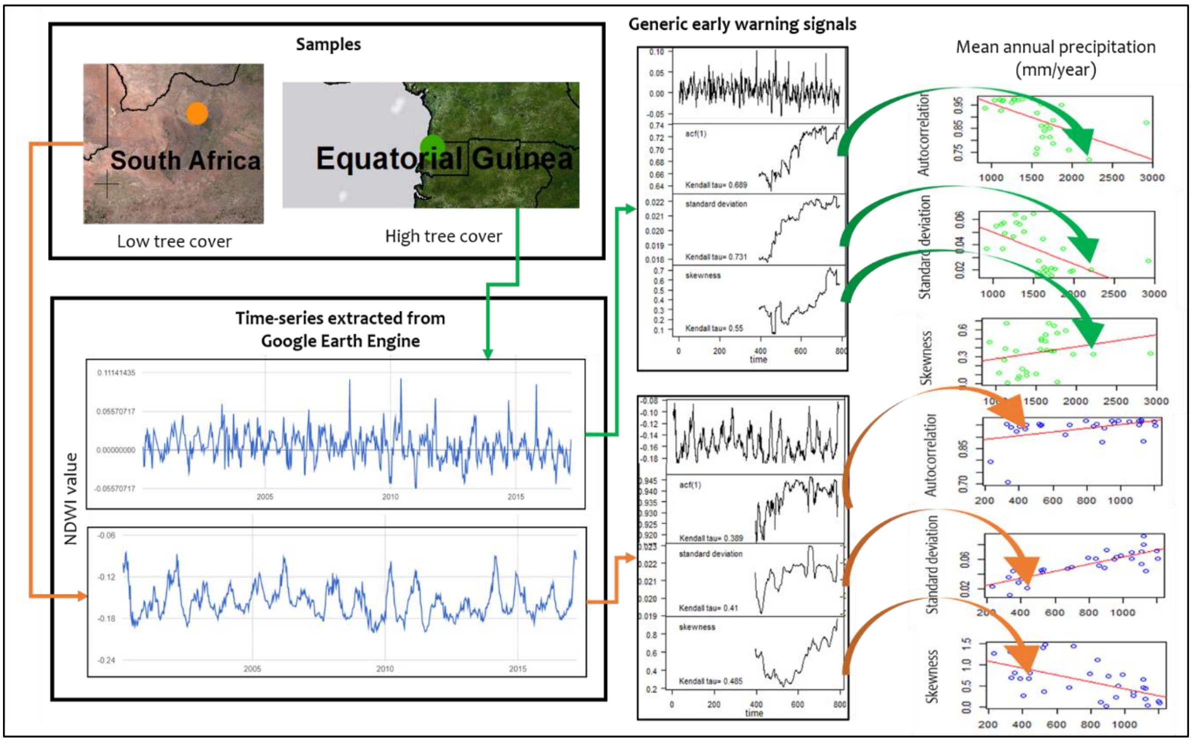

Figure 3.6. Workflow of analysis on statistical stability indicators towards increasing environmental conditions, green arrows represent flow of the processes in high tree cover while orange arrows mark those in low tree cover; green points are the sample units with high tree cover while blue points are with low tree cover

Figure 3.6. summarizes all the steps executed for the second objective of this study in a workflow. It started with selecting 60 samples in total for both distinct biome states (high and low tree cover) through a random selection. A forest ecosystem in Equatorial Guinea was exemplified in Figure 3.6. for high tree cover and a savanna in South Africa for low tree cover. Temporal dynamics of biome state indicators (NDWI, NDVI and LST) were extracted in Google Earth Engine with the extent of areas covered by trees on each sample unit of TREES data. Subsequently, a process called 'generic early warning signals' in R-environment was done to compute the values of statistical stability indicators (autocorrelation, standard deviation and skewness) on each sample unit with tree cover extent. Finally, the values of each statistical stability indicator in 30 locations (sample units) on each biome state were plotted against the environmental conditions that regulate those locations (mean annual precipitation, coefficient of variation of annual precipitation and total fire count).

4. RESULTS

4.1. Analysis on bistability under environmental conditions

The strongest concentration of areas with high tree cover was found in the centre of Sub-Saharan Africa (Figure 4.1a). High tree cover extents, composed by humid dense forests, lied in the Congo basin and spread into the Miombo woodlands (ranging between Angola and Tanzania). These were also predominant in Madagascar. The northern part of Sub-Saharan Africa is dominated by deserts lying around the Sahel belt, with zero percent of tree cover extent. The southern region is occupied by desert, agriculture and grasslands. The spatial distribution of tree cover and environmental drivers in Sub-Saharan Africa at 10x10 km basis is presented in Appendix 1.

Frequent fire counts were discovered along the horizontal line above the equator and between Angola and Tanzania, depicted by Figure 4.1.b. The pattern of spatial distributions between tree cover and fire occurrence were similar in the centre of the continent, where fire occurrence is zero and tree cover is high. This suggests a negative influence of fire occurrence to tree cover, that was also supported by the spatial distribution of low tree cover in between Angola and Tanzania, where frequent fires were detected. However, there were several areas with high tree cover found under high level of fire occurrence.

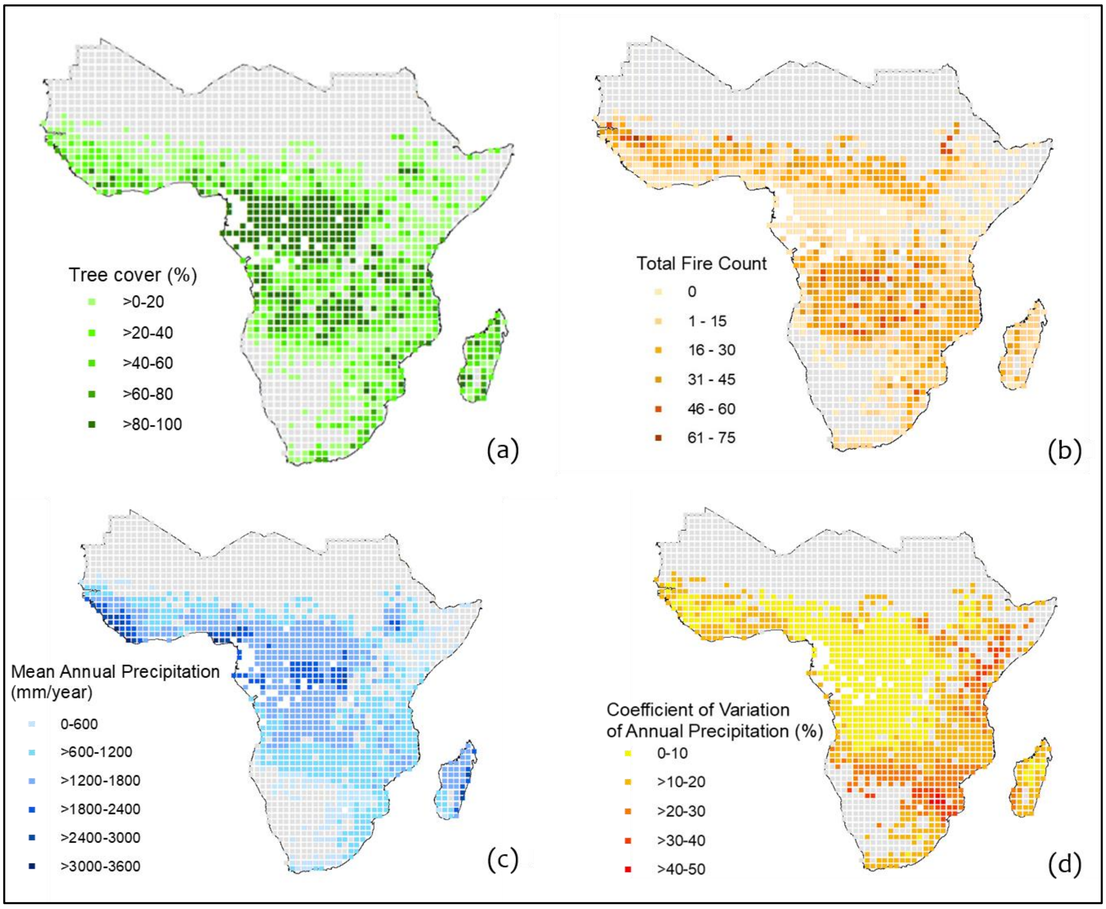

Figure 4.1. Spatial distribution of tree cover percentage calculated from TREES data (a), total fire count from MCD45A1 MODIS monthly burned-area product (b), mean and coefficient of variation of annual precipitation from CHIRPS data (c and d) within 10 years (2000-2010) on areas covered by trees

Even though forests were mostly found in the center of Sub-Saharan Africa at which precipitation reaches its highest level (Figure 4.1.c) and high precipitation in Madagascar corresponds to its tree cover distribution, in general, the influence of precipitation on the spatial distribution of tree cover was not so clear, compared to fire. Instead, spatial distribution of precipitation showed inverse relationship to fire in some locations, e.g. in the north-western part (Senegal, Guinea, Sierra Leone and Liberia) shown in dark blue by Figure 4.1.c, and between Angola and Tanzania.

Figure 4.1.d implies how precipitation amount varied over time during the observation period (2000-2010) through an analysis on coefficient of variation of annual precipitation. The largest variability of precipitation was found mostly in the East African coastal areas. The influence of spatial distribution of precipitation variability to tree cover was shown by the existence of forest in Central Africa and the prevalence of low tree cover, rather than high tree cover, along the East African coastal lines. However, despite large precipitation variability in Madagascar, forests were still predominant under its coastal climate.

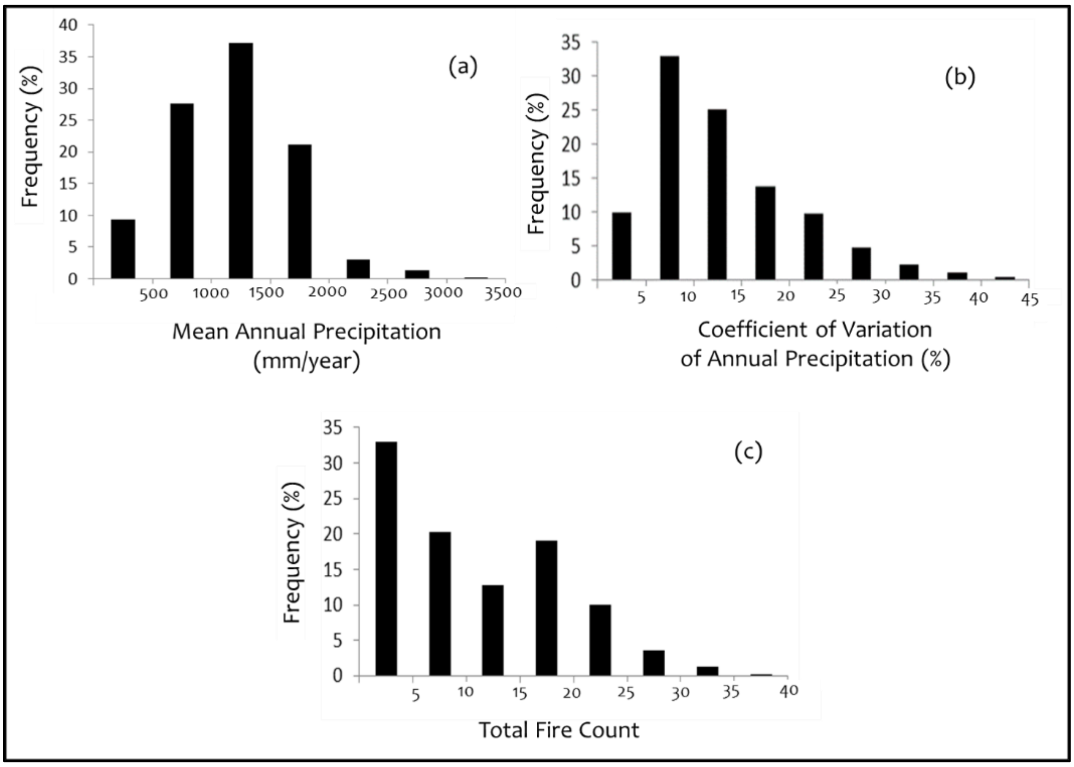

Figure 4.2. Relative frequency distribution of observed environmental drivers: precipitation (a and b) and fire (c) between 2000 and 2010 on areas covered by tree

The relative frequency distribution of mean annual precipitation was similar with that of coefficient of variation of annual precipitation on areas covered by trees, with a peak in the value range (Figure 4.2). Mean annual precipitation had normal distribution, suggesting that areas covered by trees in Sub-Saharan Africa were mainly regulated under intermediate level of mean annual precipitation. Meanwhile, coefficient of variation of annual precipitation had skewed distribution to the left of the histogram, indicating that the precipitation variability on tree cover area was relatively small. The frequency distribution of fire occurrence showed two peaks, indicating bimodal distribution. Fire histogram represents two classes: low (0-10 fire count) and high level of fire occurrence (>10 fire count).

For further analysis on the ranges of environmental condition where two distinct biome states occur (bistability), this study split the histograms presented by Figure 4.2. into smaller classes depending on their bin ranges: 500 mm/year for mean annual precipitation, 5% for coefficient of variation of annual precipitation and 5 occurrences for total fire count. The frequency distributions of tree cover on observed environmental drivers (Figure 4.3.) showed bimodal patterns, except at mean annual precipitation of 0-1000 mm/year and at higher level of coefficient of variation of annual precipitation (>25%), where each range was dominated by either low or high percentage of tree cover. The distribution of each observed environmental driver across its gradients showed two maxima of low (<5%) and high tree cover percentage (>95%), representing the existence of two distinct biome states through bimodality. The areas with intermediate tree cover between those two peaks were rare at low to intermediate level of observed environmental drivers. The midpoint along tree cover axis with minimum frequency of tree cover that split both biome states tended to be consistent, despite unclear separation (60% for all the observed environmental drivers).

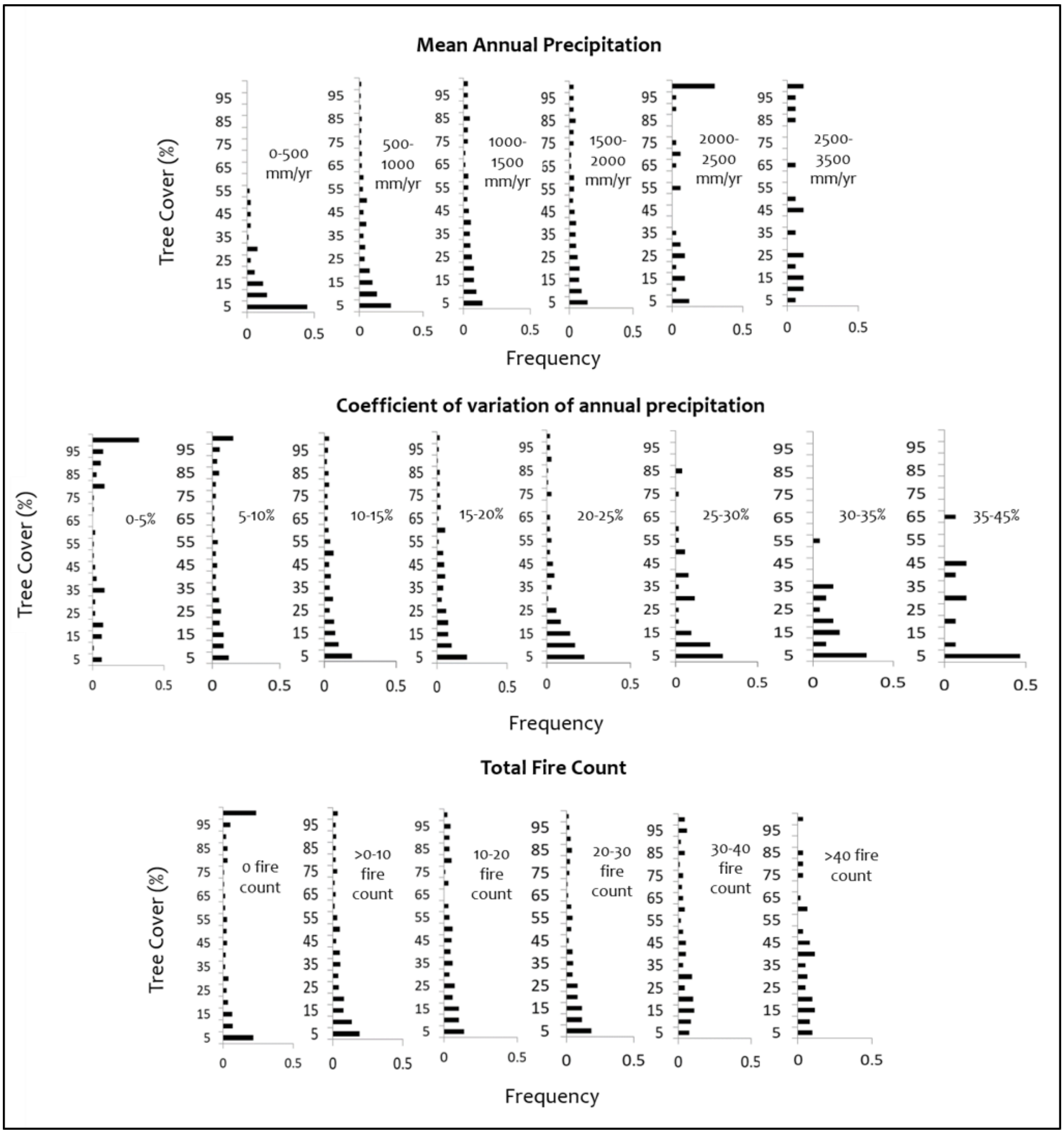

Figure 4.3. Frequency distributions of tree cover percentage at different ranges of environmental drivers, indicating two distinct African biome states through bimodalilty: savanna and forest characterized by low and high tree cover respectively

Rather than an obvious threshold of environmental condition that regulates savanna, Figure 4.3. suggests the existence of savanna at any level of observed environmental drivers. In contrast, it was apparent that forests start growing at mean annual precipitation of >500 mm/year. Despite that a high tree cover was observed for low precipitation amount (between 500 and 1000 mm/year) in a few instances, these areas were very rare and the overall distribution between 0-1000 mm/year did not provide a clear indication of bistability. The distinct frequency between both biome states persisted with increasing precipitation at up to 2500 mm/year. A gradual increase on tree cover percentage along mean annual precipitation gradient turned to a shifting occurrence of both biome states at >2500 mm/year, as forest and savanna were evenly distributed.

When looking at annual precipitation variability, it was found that high tree cover (>75%) was dominant for low coefficient of variation (up to 10%) shown by Figure 4.3. and it seems to switch to lower states after the gradient goes above 10%. The overall forest distribution on coefficient of variation of annual precipitation suggests more obvious determination where forest could specifically occur (which is at <25%), compared to savanna. Savanna was present at any level of coefficient of variation while forest extremely became scarce at >25%. However, the frequency distribution of savanna increased with increasing gradient of precipitation variability. In contrast, once the level of precipitation variability became >5%, forest presence decreased along the increasing gradient, which persisted with low frequency at 10-25% until it was very rare at >25% and suddenly absent at >30%.

The presence of savanna that persisted along the increasing fire count gradient indicates that savanna occurs more often than forests when fires are present, while forest had a considerable drop in frequency and subsequently persisted with low frequency, once it fell under fire occurrence of >0 Figure 4.3.). There were only few forests occurred at >0 fires until forests suddenly became uncommon at >40. This suggests that fire prone conditions were less suitable for forests (>0 up to 40). This also happened on savanna along the gradient of fire occurrence, that there was a decrease in frequency at >30 fire count.

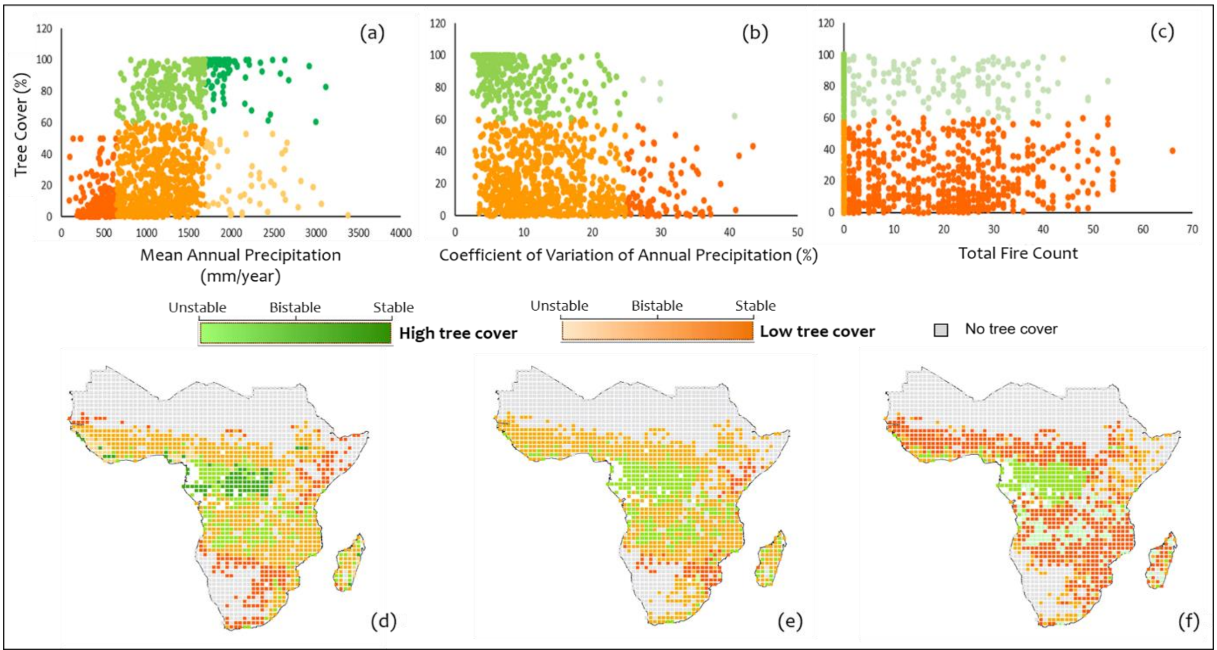

Figure 4.4. Relationships between tree cover percentage and environmental drivers (a, b, and c) and their spatial distributions (d, e, and f), illustrating condition of bistability: >650 mm/year for mean annual precipitation, 0-25% for coefficient of variation of annual precipitation and zero fire count. Sample units with tree cover of >60% are indicated in green and those with tree cover of <60% in orange. The level of stability increases with decreasing brightness in both colors.

Figure 4.4.(a-c) confirms that bistability was detected on the relationship between tree cover and each environmental driver. The midpoints along tree cover axis on the observed environmental drivers were consistent, thus to further evaluate the condition of bistability, this study defines 60% as a threshold to separate between high and low tree cover percentage. This threshold was defined based on the pattern of tree cover frequency distribution on each environmental driver, showing similar midpoints among different environmental drivers, to distinguish between distinct biome states (shown by Figure 4.3.). Areas with condition of bistability were defined in the value range at >650 mm/year for mean annual precipitation, at <25% for coefficient of variation of annual precipitation and at zero fire count.

The range of condition of bistability on mean annual precipitation (figure 4.4.a) obviously separated savanna from forest. Savanna dominated at mean annual precipitation of <650 mm, while forests were absent. Figure 4.4.b shows that areas with condition of bistability were found under low to intermediate level of precipitation variability (up to 25%). Identification of areas with condition of bistability on precipitation variability was apparent, as the existence of forest and the frequency of savanna was found to correspond to the increasing gradient of precipitation variability. When the precipitation variability was >25%, forests were infrequent. A rare case on the occurrence of forest at >25% of coefficient of variation suggests that these forests were unstable, as mostly savannas were expected to be present. Under fire occurrence, when the fire count goes above zero, it seems that mainly the biome states are savannas and not forests. Thus, forests at >0 fire count were classified as unstable. There was no clear threshold to define the absence of forest due to fire occurrence, despite a slight decrease of tree cover percentage at fire count of >45.

Figure 4.5. presents the results of analysis on bistability under all the observed environmental conditions. There were no forests considered as consistently stable based on the analysis shown in Figure 4.4. Despite several stable forests found under mean annual precipitation, these forests were classified as bistable under coefficient of variation of annual precipitation and total fire count (Figure 4.4.(d-f)). Meanwhile, the persistent stable savannas were found in the southern part of Sub-Saharan Africa, lying in a horizontal line from Namibia to Mozambique.

Bistable forests under all the observed environmental drivers were found mostly in the Congo basin, spreading to Angola and Zambia. Scattered points of bistable forests were also found in Madagascar, Kenya and Tanzania. Along the north-western coastal lines (from Ivory Coast to Nigeria), bistable forests were adjacent to bistable savannas. Other bistable savannas spread along the eastern part of Sub-Saharan Africa, from Ethiopia to South Africa. Some of them lied also in the zone surrounding the Congo basin and in Madagascar.

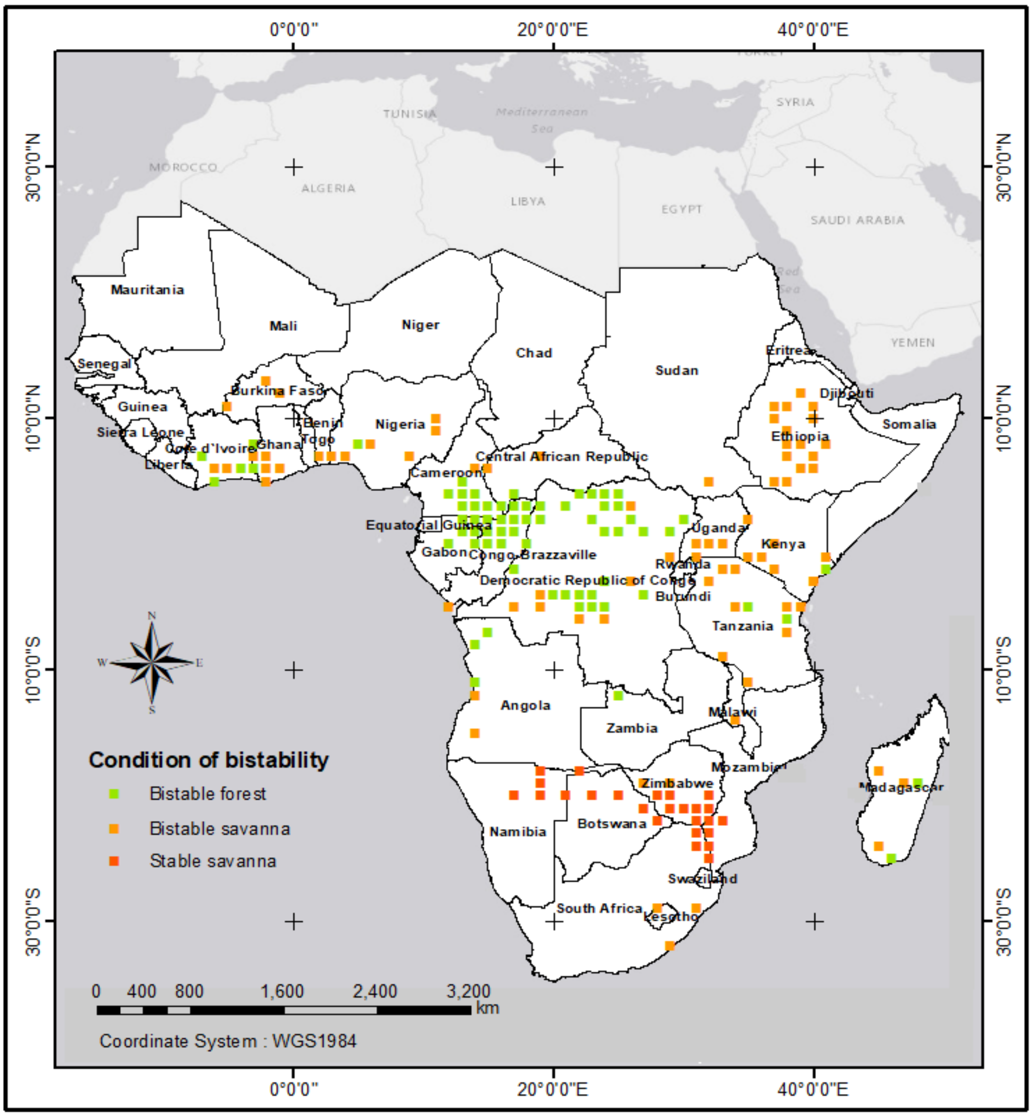

Figure 4.5. Spatial distribution of bistable biome states under three observed environmental drivers (mean annual precipitation, coefficient of variation of annual precipitation and total fire count)

4.2. Analysis on statistical stability indicators on distinct biome states

Figure 4.6. presents the trends on autocorrelation, standard deviation and skewness as statistical stability indicators to indicate instability on two locations of distinct biome states. The upper windows are the temporal dynamics of NDWI in linear detrending. NDWI values in high tree cover (A) were higher than those in low tree cover (B).

The positive trends showed in all the statistical stability indicators by Figure 4.6. were expected to appear if the biome states undergo critical transitions, as there is a slowing down process of their recovery rate (Dakos et al., 2012). Thus, these two locations could be considered to possibly experience slowing down process within the observation period (2000-2017), based on those similar increasing patterns in the statistical stability indicators.

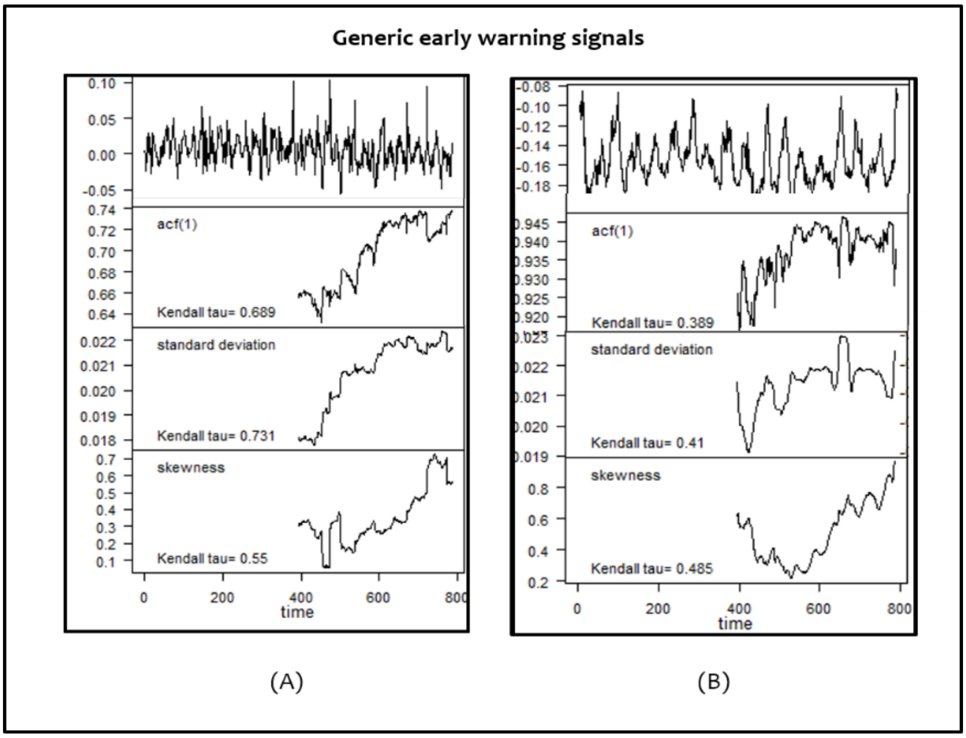

Figure 4.6. Time series profiles of NDWI on an area with high tree cover located at 2^0 N and 10^0 E (A) and an area with low tree cover located at 27^0 S and 24^0 E (B)

Figure 4.7. – 4.9. and Appendix 2 show changes in each statistical stability indicator along changing environmental conditions in different detrending techniques. Generally, with increasing mean annual precipitation, rises in the values of statistical stability indicators were found on high tree cover, while decreases were on low tree cover. Opposite patterns to those on mean annual precipitation were towards increasing coefficient of variation of annual precipitation. There were increases on both distinct biome states with increasing fire occurrence. These patterns on the observed environmental drivers were similar among all the detrending techniques applied.

The signs of bistability on autocorrelation generally corresponded to the expected direction (Figure 4.7. – 4.9.). Autocorrelation of all the biome state indicators were significant on high tree cover in linear detrending and gaussian filtering (Table 4.2.). Skewness seems to behave inversely towards changing environmental conditions, compared to autocorrelation and standard deviation. Standard deviation of NDVI on high tree cover showed opposite patterns to other statistical stability indicators. This was consistent under all the observed environmental drivers that standard deviation tended to show no change in NDVI value.

Compared to other biome state indicators, LST performed unexpected direction of changes of all the statistical stability indicators on low tree cover, shown by Figure 4.7. – 4.9. With increasing mean annual precipitation on low tree cover, LST shows decreases rather than increases, while it tended to remain constant with increasing fire. Meanwhile, NDWI was found to have more corresponding signs of bistability to what were expected. However, despite different patterns found, all the statistical stability indicators of LST under precipitation condition were always significant in any detrending techniques (Table 4.2.). Surprisingly, in first-differencing, significant trends of LST were under all the observed environmental conditions on high tree cover.

Appendix 2 shows similar direction of changes in the values of statistical stability indicators among different detrending techniques. Nevertheless, there were different direction of changes discovered on standard deviation of NDVI and LST in first-differencing filtering. However, despite several unexpected direction of changes, based on the significance, statistical stability indicators of NDVI show most significant trends in first-differencing. Meanwhile, for other detrending techniques, most significant trends were detected for statistical stability indicators derived from NDWI, followed by NDVI, while LST produced less significant trends, shown by Table 4.2.

The highest variance explained on the regression analysis was in standard deviation of NDWI on low tree cover under precipitation condition (Table 4.2.). This value was similar with that in any different detrending techniques, except for first-differencing filtering (Appendix 3). In first-differencing, R^2 value of NDWI autocorrelation under fire occurrence was the highest.

Table 4.1. R^2 and trend significance between tree cover and environmental drivers in linear detrending, with significance level: *** p<0.001; ** p<0.01; * p<0.05, p<0.1

Environmental driver	Tree cover (%)	Statistical stability indicators	NDWI	NDVI	LST
Mean annual precipitation	High	Autocorrelation	0.34***	0.50***	0.49***
		Standard deviation	0.34***	0.00	0.52***
		Skewness	0.09	0.06	0.46***
	Low	Autocorrelation	0.19*	0.04	0.05
		Standard deviation	0.69***	0.50***	0.07
		Skewness	0.35***	0.47***	0.17*
Coefficient of variation of annual precipitation	High	Autocorrelation	0.22**	0.33***	0.52***
		Standard deviation	0.09	0.10	0.08
		Skewness	0.05	0.24**	0.07
	Low	Autocorrelation	0.08	0.01	0.13
		Standard deviation	0.49***	0.36***	0.12
		Skewness	0.15*	0.27**	0.21*
Total fire count	High	Autocorrelation	0.51***	0.56***	0.59***
		Standard deviation	0.67***	0.06	0.12
		Skewness	0.23**	0.11	0.09
	Low	Autocorrelation	0.18*	0.15*	0.02
		Standard deviation	0.38***	0.47***	0.01
		Skewness	0.06	0.11	0.00

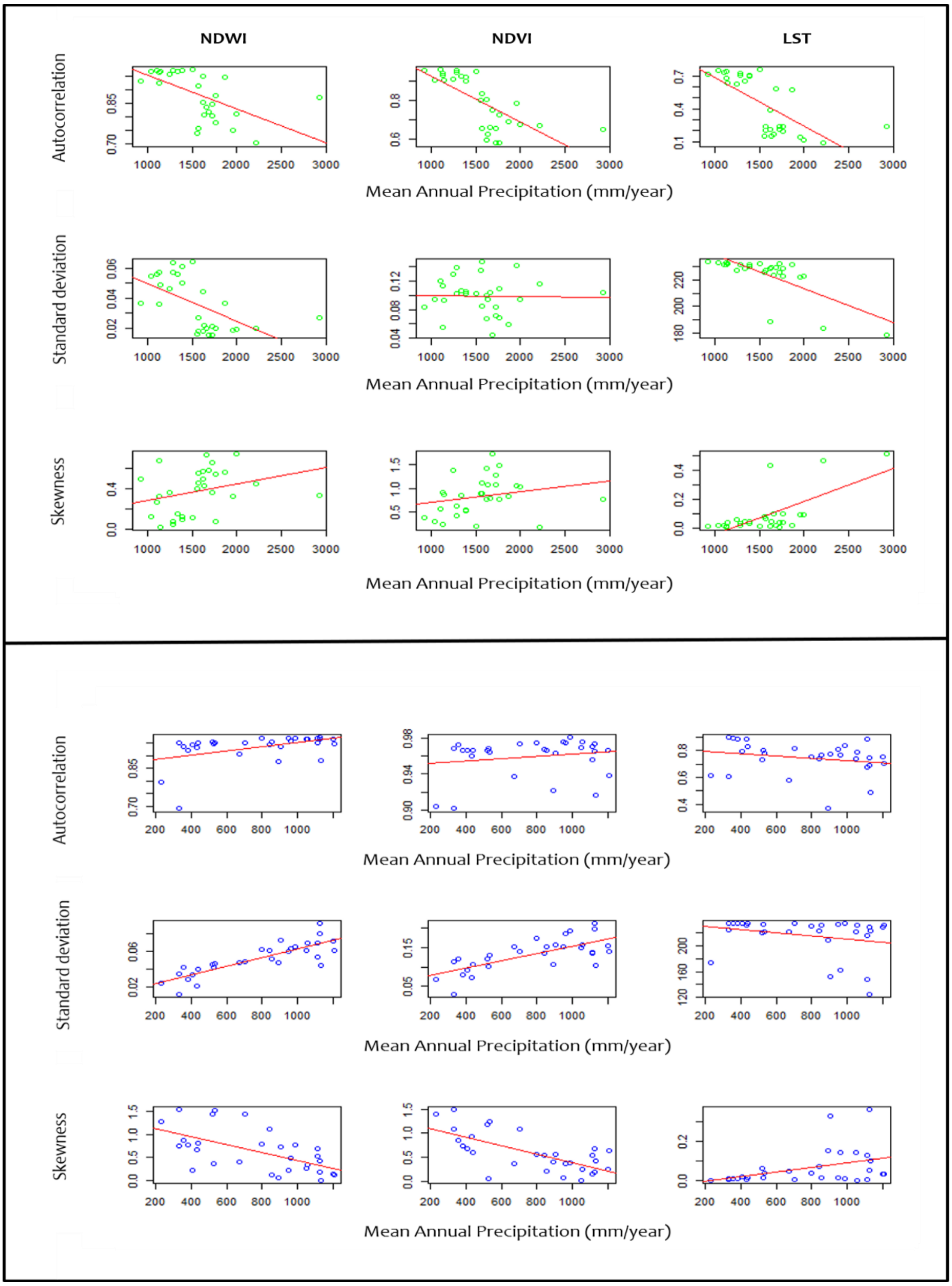

Figure 4.7. Regression analysis on mean annual precipitation in linear detrending

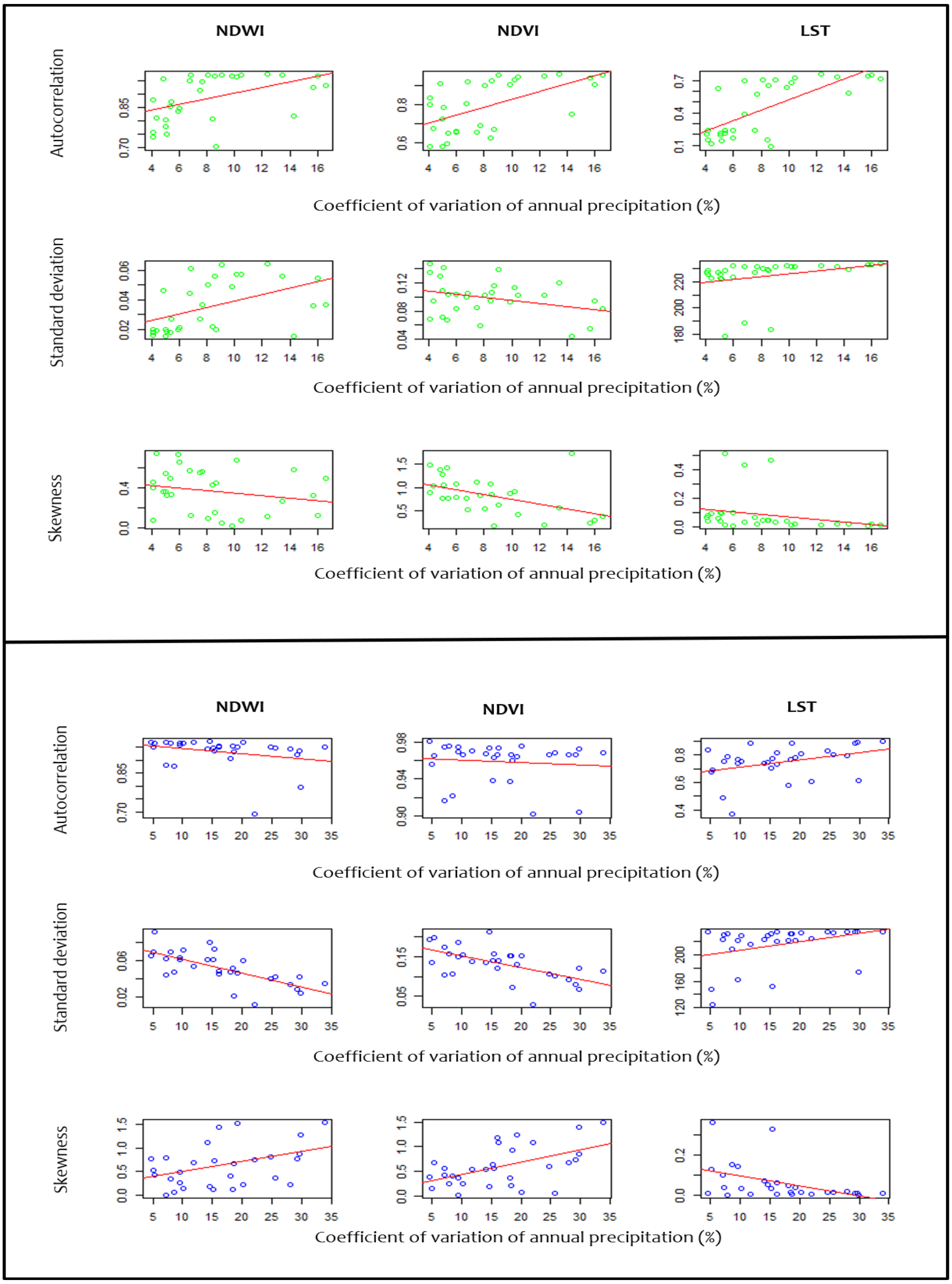

Figure 4.8. Regression analysis on coefficient of variation of annual precipitation in linear detrending

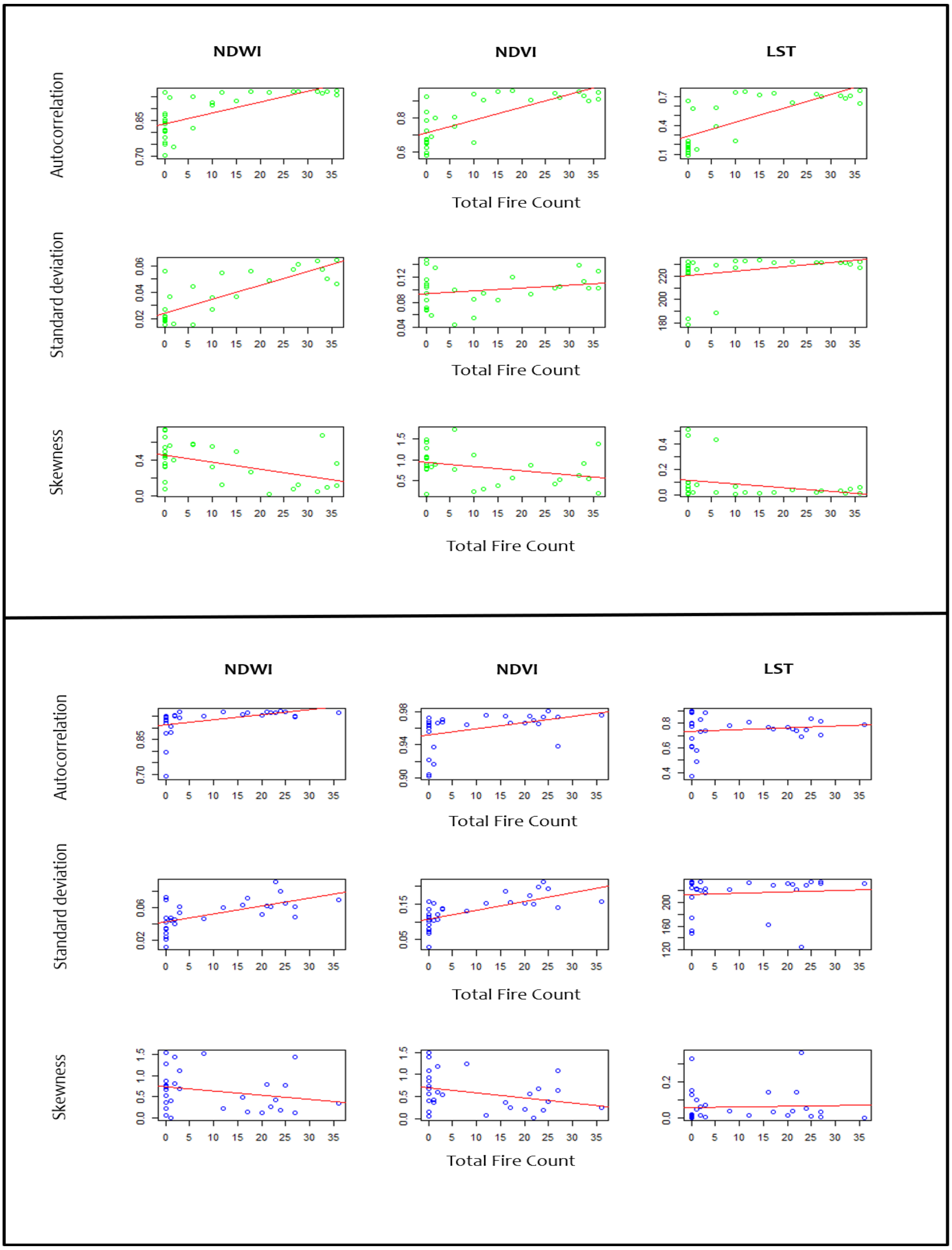

Figure 4.9. Regression analysis on total fire count in linear detrending on distinct biome states; high tree cover in green and low tree cover in blue

5. DISCUSSION

5.1. Analysis on bistability under environmental conditions

The frequency distributions of all the observed environmental drivers in this study suggest that forest and savanna (high and low tree cover) might become alternative stable states at the value ranges where bistability occurs: >650 mm/year for mean annual precipitation, 0-25% for coefficient of variation of annual precipitation and zero fire count. Analysis on bistability under certain environmental conditions is of importance, as potential window of opportunity for restoration efforts could be developed to reduce the risks of critical transitions to alternative stable states (Hirota et al., 2012). Alternative stable state reached after perturbation might be undesirable, thus understanding the underlying mechanisms of bistability could help to anticipate such critical transitions to happen (Kéfi et al., 2007).

The spatial distribution shown by Figure 4.5. suggests the potential changes on biome states, either at the cost of forest or savanna. Surprisingly, under all the observed environmental drivers, bistable forests were discovered in the Congo Basin, that seemed to be persistent and were considered to experience a slight change over a long time. This might need further evaluation on the temporal dynamics of these forest ecosystems in a longer time series period or on observations under other drivers to conclude if potential critical transitions to alternative stable states could really occur on these bistable forests. On the other hand, the loss of savanna suggests the expansion of forest ecosystems, which in this case, alternative stable states are more desirable.

Despite the same study area, bistability determination in this study was different from the previous studies by Staver et al. (2011a) and Hirota et al. (2012). Different datasets used might be a possible explanation for the difference between the patterns of bistability found in this study and in those studies. Both prior studies analyzed tree cover data on MODIS Vegetation Continuous Field (VCF) dataset, which has a spatial resolution of 250 m. Compared to TREES data, which are derived from a Landsat pixel of 30 m, mapping accuracy in tree cover density on MODIS-VCF might be lower than TREES data, as mixed vegetation cover could be more possibly found in larger spatial resolution, affecting confusion in the classification process on the spectral signature. This was also confirmed by Townshend et al. (2011) and Sexton et al. (2013), through a quality control on root mean square errors (RMSE) of MODIS-VCF, that the largest RMSE value was in a mixed forest or a mixed agriculture landscape.

Besides tree cover data, the methods for calculating tree cover also constituted different results. The calculation of tree cover percentage in this study was not based on the size of the sample unit of TREES data (10 x 10 km), but on the size of natural area on each sample, consisting of TC, TCM and other wooded land. This aimed to exclude areas of human interventions (agriculture and settlements) from analysis on tree cover, because a small tree cover in a sample unit could rather be influenced by human interventions, instead of environmental drivers. In consequence, this led to abundance of sample units with 100% tree cover, as these sample units only have TC or TCM area (without any areas of other wooded land). However, this resulted in the exclusion of another land cover class as well, i.e. grasslands, from the classified natural areas, as grassland and agriculture were not separated into different classification in TREES data. This might have created some bias in excluding too much grasslands in this study. In that way, tree cover percentage could have been calculated higher in this study than it would have been in its real condition.

5.2. Analysis on statistical stability indicators on distinct biome states

This study found that the statistical stability indicators (autocorrelation, standard deviation and skewness) of remotely-sensed biome state indicators (NDVI, NDWI and LST) showed changes in a beforehand-anticipated direction towards changing environmental conditions. The direction of changes in statistical stability indicators was generally similar among different detrending techniques. However, opposite direction of changes in statistical stability indicators was found in skewness with all the detrending techniques and standard deviation of NDVI and LST in high tree cover with first-differencing filtering.

Autocorrelation was found as more responsive statistical stability indicator in showing bistability, compared to skewness and standard deviation, as it showed more corresponding signs of bistability to what were expected. Compared to autocorrelation and standard deviation, skewness showed opposite direction of change on both high and low tree cover under all the observed environmental drivers. Rather than a decrease on high tree cover, the positive skewness under mean annual precipitation occurred as the probability density distribution is higher at the right tail of the datasets or at the large end of the distribution than at the left tail or the small end (He et al., 2013). The datasets may display skewness in opposite direction to what was expected due to the fact that the time series is not long enough to properly estimate skewness. Hence, skewness was not considered as responsive to indicate instability towards changing environmental conditions in this study.

Even though detrending was applied to tackle seasonality issue, the effect of seasonality on time series could not be completely removed, as standard deviation mostly showed relatively constant patterns with only a slight decrease or increase. The detrending techniques applied in this study were considered to only filter out the seasonality partially, as standard deviation of NDVI in high tree cover showed no change or sometimes increased and it was consistent among different detrending techniques. However, this issue could be also because there is less likely high variation in greenness level in dense forest. This could be related to saturation, as in tropical forest NDVI tends to saturate to high values and the variation would be very little.

Based on the performance in indicating instability, all the detrending techniques applied were considered insufficient, despite that gaussian filtering was expected to be the most appropriate technique to indicate instability. Those detrending techniques could not completely cope with non-stationarity in the time series, in the case of standard deviation of NDVI. Compared to first-differencing, gaussian filtering and linear detrending could better perform the signs of bistability. In first-differencing, LST had different direction of changes in standard deviation from what was expected. This could happen as each successive differencing could decrease the variance of the series, affecting the standard deviation as well, but at the same time, it could also lead to an increase in variance (Lenton et al., 2012). The issues on detrending techniques might be overcome by defining appropriate parameter choices (e.g. filtering bandwidth, sliding window length, degree of smoothing), to improve the performance of statistical stability indicators and remotely-sensed biome state indicators in indicating instability.

The decreases of the values of statistical stability indicators of NDVI and NDWI on low tree cover could happen as the tree growth decreases with increasing precipitation variability, thus large precipitation variability would not stimulate transitions to higher tree cover. In other words, the biome states would persist as savannas or areas with low tree cover. Compared to NDWI and NDVI, LST behave inversely in all the statistical stability indicators under increasing mean and coefficient of variation of annual precipitation on low tree cover. This might happen as LST plays contrasting role than NDWI and NDVI in explaining ecosystem instability. Lower tree cover percentage is associated to lower values of NDWI and NDVI, thus on low tree cover with increasing precipitation, instability could be detected on NDWI and NDVI by showing increases, implying transitions to higher tree cover or forests. In contrast, higher LST value often characterizes low tree cover percentage. This might affect the patterns to show no transitions to higher tree cover or forests, as decreases were found on low tree cover with increasing precipitation. Otherwise, this case could either indicate failed detections or false negatives, where transitions are expected to happen (Alibakhshi et al., 2017). Thus, if false negative is the case, LST could be considered as unreliable in explaining ecosystem instability. More corresponding patterns between observation and hypothesis were found on NDWI, among all the biome state indicators. This was also shown by more significant results on NDWI from its p-values. Therefore, NDWI was considered as the most relevant biome state indicator in indicating instability in this study.

Uncertainties found in explaining ecosystem instability were classified into false signals and failed detections. False signals (false positive) are mostly caused by changes in the stochastic regime of perturbations, a factor other than the actual dynamics (Scheffer et al., 2009; Dakos, Nes, Odorico, & Scheffer, 2016). Extreme events (in this study is exemplified by frequent fire occurrence) could cause ecosystem to be more liable to change, due to increases in the magnitude of environmental stochasticity (Dakos et al., 2014). This, in turn, would affect the statistical stability indicator to indicate transitions. Therefore, in this case, due to fire occurrence, transitions on low tree cover indicate false signals (false positive). However, the absence of the signals to warn such transitions would also be disastrous (Dakos et al., 2014). Periodically fluctuating environmental conditions (i.e. shown by LST and standard deviation of NDVI under seasonality) might result in no transitions shown by the statistical stability indicators (Carpenter and Brock, 2010). Nonlinearity condition on standard deviation of NDVI could also cause false negative, at which the ecosystem is not in equilibrium prior to critical transitions (Drake and Griffen, 2010). Hence, detection of warning signals could be more challenging. This issue could be tackled if there are adequate baseline data as reference for calibration.

6. CONCLUSIONS AND RECOMMENDATIONS

6.1. Conclusions

- In this study, the frequency distributions of all the observed environmental drivers suggest that forest and savanna (high and low tree cover) might become alternative stable states at the value ranges where bistability occurs: >650 mm/year for mean annual precipitation, 0-25% for coefficient of variation of annual precipitation and zero fire count.

- The statistical stability indicators (autocorrelation, standard deviation and skewness) of remotely-sensed biome state indicators (NDVI, NDWI and LST) showed changes in a beforehand-anticipated direction towards changing environmental conditions. The direction of changes in statistical stability indicators was generally similar among different detrending techniques.

- The performance of biome state indicators, detrending techniques and statistical stability indicators in indicating instability was assessed. NDWI was considered as the most relevant biome state indicator and autocorrelation was the most responsive statistical stability indicator in indicating instability in this study. However, all the detrending techniques applied were considered insufficient, as they could not completely cope with non-stationarity issue in the time series.

6.2. Recommendations for future studies

- The analysis on how statistical stability indicators explain the potential instability on biome states could be improved with ancillary data, proper methods on time series analysis, sensitive biome states indicators and relevant observed environmental drivers. These factors are considered essential for more satisfactory outputs in observations on bistability and time series analysis in the future.

- Potential use of TREES data was proven by previous studies, compared to other tree cover data (e.g. MODIS-VCF and GFC). However, an improvement is needed so as to deal with projection issues on TREES data. Tedious work on manual process of defining the original projection of TREES data should be reduced. Also, an appropriate projection system should be considered in order to avoid bias on tree cover estimates. The availability of ground-truth data about the conditions and temporal dynamics of biome states could also contribute to improve the results of analysis on ecosystem instability.

- In applying detrending techniques, it is crucial to define appropriate parameter choices (e.g. filtering bandwidth, sliding window length, degree of smoothing), as this might constitute to better results in indicating instability. By properly detrending time series data, the performance of statistical stability indicators and remotely-sensed biome state indicators could possibly be improved.

LIST OF REFERENCES

Achard, F., Beuchle, R., Mayaux, P., Stibig, H.-J., Bodart, C., Brink, A., Carboni, S., Desclée, B., Donnay, F., Eva, H.D., Lupi, A., Raši, R., Seliger, R., Simonetti, D., 2014. Determination of tropical deforestation rates and related carbon losses from 1990 to 2010. Glob. Chang. Biol. 20, 2540–2554. https://doi.org/10.1111/gcb.12605

Alibakhshi, S., Groen, T.A., Rautiainen, M., Naimi, B., 2017. Remotely-Sensed Early Warning Signals of a Critical Transition in a Wetland Ecosystem. https://doi.org/10.3390/rs9040352

Beisner, B., Haydon, D., Cuddington, K., 2003. Alternative stable states in ecology. Front. Ecol. Environ. 1, 376–382. https://doi.org/10.1890/1540-9295(2003)001[0376:ASSIE]2.0.CO;2

Biggs, R., Carpenter, S.R., Brock, W.A., 2009. Turning back from the brink: Detecting an impending regime shift in time to avert it. Proc. Natl. Acad. Sci. 106, 826–831. https://doi.org/10.1073/pnas.0811729106

Bodart, C., Brink, A.B., Donnay, F., Lupi, A., Mayaux, P., Achard, F., 2013. Continental estimates of forest cover and forest cover changes in the dry ecosystems of Africa between 1990 and 2000. J. Biogeogr. 40, 1036–1047. https://doi.org/10.1111/jbi.12084

Carpenter, S.R., Brock, W.A., 2010. Early warnings of regime shifts in spatial dynamics using the discrete Fourier transform. Ecosphere 1, 1–15. https://doi.org/10.1890/ES10-00016.1

Dakos, V., Carpenter, S.R., Brock, W.A., Ellison, A.M., Guttal, V., Ives, A.R., Ké Fi, S., Livina, V., Seekell, D.A., Van Nes, E.H., Scheffer, M., 2012. Methods for Detecting Early Warnings of Critical Transitions in Time Series Illustrated Using Simulated Ecological Data. PLoS One 7. https://doi.org/10.1371/journal.pone.0041010

Dakos, V., Carpenter, S.R., van Nes, E.H., Scheffer, M., 2014. Resilience indicators: prospects and limitations for early warnings of regime shifts. Philos. Trans. R. Soc. B Biol. Sci. 370, 20130263–20130263. https://doi.org/10.1098/rstb.2013.0263

Dakos, V., Nes, E.H. Van, Odorico, P.D., Scheffer, M., 2016. Robustness of variance and autocorrelation as indicators of critical slowing down Author (s): Vasilis Dakos , Egbert H . van Nes , Paolo D â€™ Odorico and Marten Scheffer Published by : Wiley Stable URL : http://www.jstor.org/stable/23143907 REFERENCES Li 93, 264–271.

Dakos, V., Scheffer, M., Nes, E.H. van, Brovkin, V., Petoukhov, V., Held, H., 2009. Slowing down as an early warning signal for abrupt climate change. IOP Conf. Ser. Earth Environ. Sci. 6, 62012. https://doi.org/10.1088/1755-1307/6/6/062012

Dantas, V. de L., Hirota, M., Oliveira, R.S., Pausas, J.G., 2016. Disturbance maintains alternative biome states. Ecol. Lett. 19, 12–19. https://doi.org/10.1111/ele.12537

Dinku, T., 2014. Validation of the chirps satellite rainfall estimate. Seas. Predict. Hydro-climatic Extrem. Gt. Horn Africa 2014.

Drake, J.M., Griffen, B.D., 2010. Early warning signals of extinction in deteriorating environments. Nature 467, 456–459. https://doi.org/10.1038/nature09389

ESRI, 2012. ArcGIS 10.1 Projected Coordinate System Tables.

European Commission, 2015. TREES3 Download Tool [WWW Document]. URL http://forobs.jrc.ec.europa.eu/trees3/ (accessed 2.3.18).

Funk, C., Peterson, P., Landsfeld, M., Pedreros, D., Verdin, J., Shukla, S., Husak, G., Rowland, J., Harrison, L., Hoell, A., Michaelsen, J., 2015. The climate hazards infrared precipitation with stations—a new environmental record for monitoring extremes Background & Summary. https://doi.org/10.1038/sdata.2015.66

Groen, T.A., van Langevelde, F., van de Vijver, C.A.D.M., de Raad, A.L., de Leeuw, J., Prins, H.H.T., 2011. A continental analysis of correlations between tree patterns in African savannas and human and environmental variables. J. Arid Environ. 75, 724–733. https://doi.org/10.1016/j.jaridenv.2011.03.010

Gross, D., Achard, F., Dubois, G., Brink, A., Prins, H.H.T., 2017. Uncertainties in tree cover maps of Sub-Saharan Africa and their implications for measuring progress towards CBD Aichi Targets. Remote Sens. Ecol. Conserv. 1–19. https://doi.org/10.1002/rse2.52

Hansen, M.C., Krylov, A., Tyukavina, A., Potapov, P. V, Turubanova, S., Zutta, B., Ifo, S., Margono, B., Stolle, F., Moore, R., 2016. Humid tropical forest disturbance alerts using Landsat data. Environ. Res. Lett. 11, 34008. https://doi.org/10.1088/1748-9326/11/3/034008

He, W., Wan, S., Jiang, Y., Jin, H., Zhang, W., Wu, Q., He, T., 2013. Detecting abrupt change on the basis of skewness: Numerical tests and applications. Int. J. Climatol. 33, 2713–2727. https://doi.org/10.1002/joc.3624

Held, H., Kleinen, T., 2004. Detection of climate system bifurcations by degenerate fingerprinting. Geophys. Res. Lett. 31, 1–4. https://doi.org/10.1029/2004GL020972

Hirota, M., Holmgren, M., Van Nes, E.H., Scheffer, M., 2012. Global Resilience of Tropical Forest and Savanna to Critical Transitions. Science (80-.). 336, 541–541. https://doi.org/10.1126/science.1219711

Kéfi, S., Guttal, V., Brock, W.A., Carpenter, S.R., Ellison, A.M., Livina, V.N., Seekell, D.A., Scheffer, M., Van Nes, E.H., Dakos, V., 2014. Early warning signals of ecological transitions: Methods for spatial patterns. PLoS One 9, 10–13. https://doi.org/10.1371/journal.pone.0092097

Kéfi, S., Rietkerk, M., Alados, C.L., Pueyo, Y., Papanastasis, V.P., ElAich, A., De Ruiter, P.C., 2007. Spatial vegetation patterns and imminent desertification in Mediterranean arid ecosystems. Nature 449, 213–217. https://doi.org/10.1038/nature06111

Kigomo, B., 2003. Forests and woodlands degradation in dryland Africa: A case for urgent global attention [WWW Document]. URL http://www.fao.org/docrep/ARTICLE/WFC/XII/0169-B3.htm (accessed 8.16.17).

Lenton, T.M., Livina, V.N., Dakos, V., van Nes, E.H., Scheffer, M., 2012. Early warning of climate tipping points from critical slowing down: comparing methods to improve robustness. Philos. Trans. R. Soc. A Math. Phys. Eng. Sci. 370, 1185–1204. https://doi.org/10.1098/rsta.2011.0304

Malhi, Y., Adu-Bredu, S., Asare, R.A., Lewis, S.L., Mayaux, P., 2013. African rainforests: past, present and future. Philos. Trans. R. Soc. B Biol. Sci. https://doi.org/10.1098/rstb.2012.0312

Mayaux, P., Pekel, J.-F., Desclee, B., Donnay, F., Lupi, A., Achard, F., Clerici, M., Bodart, C., Brink, A., Nasi, R., Belward, A., 2013. State and evolution of the African rainforests between 1990 and 2010. Philos. Trans. R. Soc. B Biol. Sci. 368, 20120300–20120300. https://doi.org/10.1098/rstb.2012.0300

Olson, D.M., Dinerstein, E., Wikramanayake, E.D., Burgess, N.D., Powell, G.V.N., Underwood, E.C., Amico, J.A.D., Itoua, I., Strand, H.E., Morrison, J.C., Loucks, J., Allnutt, T.F., Ricketts, T.H., Kura, Y., Lamoreux, J.F., Wesley, W., Hedao, P., Kassem, K.R., 2001. Terrestrial Ecoregions of the World: A New Map of Life on Earth 51, 933–938.

Potapov, P., Hansen, M.C., Laestadius, L., Turubanova, S., Yaroshenko, A., Thies, C., Smith, W., Zhuravleva, I., Komarova, A., Minnemeyer, S., Esipova, E., 2017. The last frontiers of wilderness: Tracking loss of intact forest landscapes from 2000 to 2013. Sci. Adv. 3, e1600821. https://doi.org/10.1126/sciadv.1600821

Scheffer, M., Bascompte, J., Brock, W.A., Brovkin, V., Carpenter, S.R., Dakos, V., Held, H., Nes, E.H. Van, Rietkerk, M., Sugihara, G., 2009. Early-warning signals for critical transitions. Nature 461, 53–59. https://doi.org/10.1038/nature08227

Scholes, R.J., Archer, S.R., 1997. Tree-Grass Interactions in Savannas. Annu. Rev. Ecol. Syst. 28, 517–544. https://doi.org/10.1146/annurev.ecolsys.28.1.517

Sexton, J.O., Song, X.-P., Feng, M., Noojipady, P., Anand, A., Huang, C., Kim, D.-H., Collins, K.M., Channan, S., Dimiceli, C., Townshend, J.R., 2013. Global, 30-m resolution continuous fields of tree cover: Landsat-based rescaling of MODIS vegetation continuous fields with lidar-based estimates of error-m resolution continuous fields of tree cover: Landsat-based rescaling of MODIS vegetation continuous fields with lidar-based estimates of error. Int. J. Digit. Earth 30, 427–448. https://doi.org/10.1080/17538947.2013.786146

Staver, A., Archibald, S., Levin, S., 2011a. Tree cover in sub-Saharan Africa: Rainfall and fire constrain forest and savanna as alternative stable states. Ecology 92, 1063–1072. https://doi.org/10.1890/10-1684.1

Staver, A., Archibald, S., Levin, S., 2011b. The Global Extent and Determinants of Savanna and Forest as Alternative Biome States. Science (80-.). 334, 230–232. https://doi.org/10.1126/science.1210465

Stibig, H.-J., Achard, F., Carboni, S., Raši, R., Miettinen, J., 2014. Change in tropical forest cover of Southeast Asia from 1990 to 2010. Biogeosciences 11, 247–258. https://doi.org/10.5194/bg-11-247-2014

Townshend, J.R.., Hansen, M.C., Carroll, M., DiMiceli, C., Sohlberg, R., Huang, C., 2011. Vegetation Continuous Fields MOD44B, 2010 Percent Tree Cover. Collect. 5, Univ. Maryland, Coll. Park. Maryl. 1–12. https://doi.org/http://glcf.umiacs.umd.edu/data/vcf/

Tsela, P., Wessels, K., Botai, J., Archibald, S., Swanepoel, D., Steenkamp, K., Frost, P., 2014. Validation of the two standard MODIS satellite burned-area products and an empirically-derived merged product in South Africa. Remote Sens. 6, 1275–1293. https://doi.org/10.3390/rs6021275

Van Nes, E.H., Hirota, M., Holmgren, M., Scheffer, M., 2014. Tipping points in tropical tree cover: Linking theory to data. Glob. Chang. Biol. 20. https://doi.org/10.1111/gcb.12398

Van Nes, E.H., Scheffer, M., 2007. Slow Recovery from Perturbations as a Generic Indicator of a Nearby Catastrophic Shift. Am. Nat 169, 0–0. https://doi.org/https://doi.org/10.1086/516845

Verbesselt, J., Umlauf, N., Hirota, M., Holmgren, M., Nes, E.H. Van, Herold, M., Zeileis, A., Scheffer, M., 2016. Remotely sensed resilience of tropical forests. https://doi.org/10.1038/NCLIMATE3108

Wu, Z., Huang, N.E., Long, S.R., Peng, C.-K., 2007. On the trend, detrending, and variability of nonlinear and nonstationary time series. Proc. Natl. Acad. Sci. 104, 14889–14894. https://doi.org/10.1073/pnas.0701020104

APPENDICES

Appendix 1

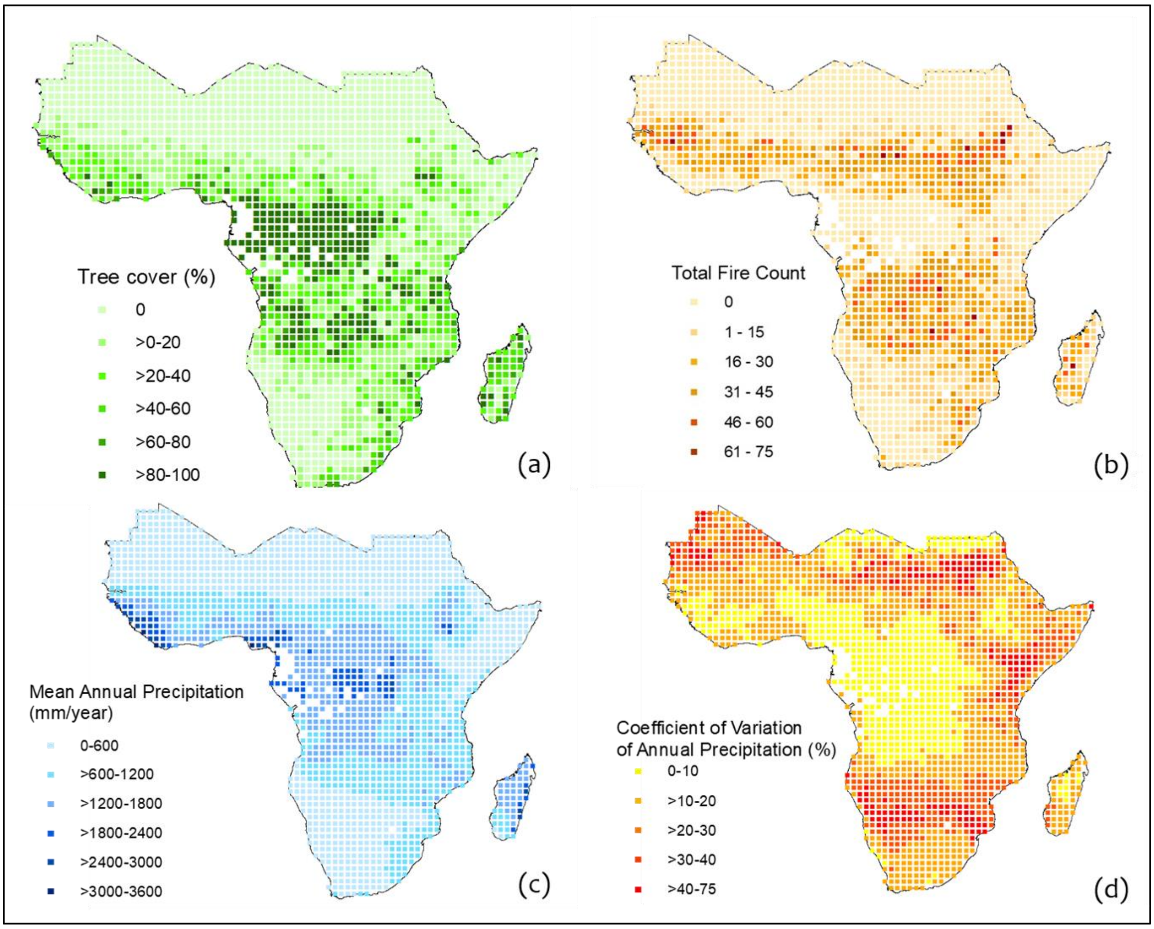

Figure A1. Spatial distribution of tree cover percentage calculated from TREES data (a), total fire count from MCD45A1 MODIS monthly burned-area product (b), mean and standard deviation of annual precipitation from CHIRPS data (c and d) within 10 years (2000-2010) over Sub-Saharan Africa at sample unit basis (10x10 km)

Appendix 2-1

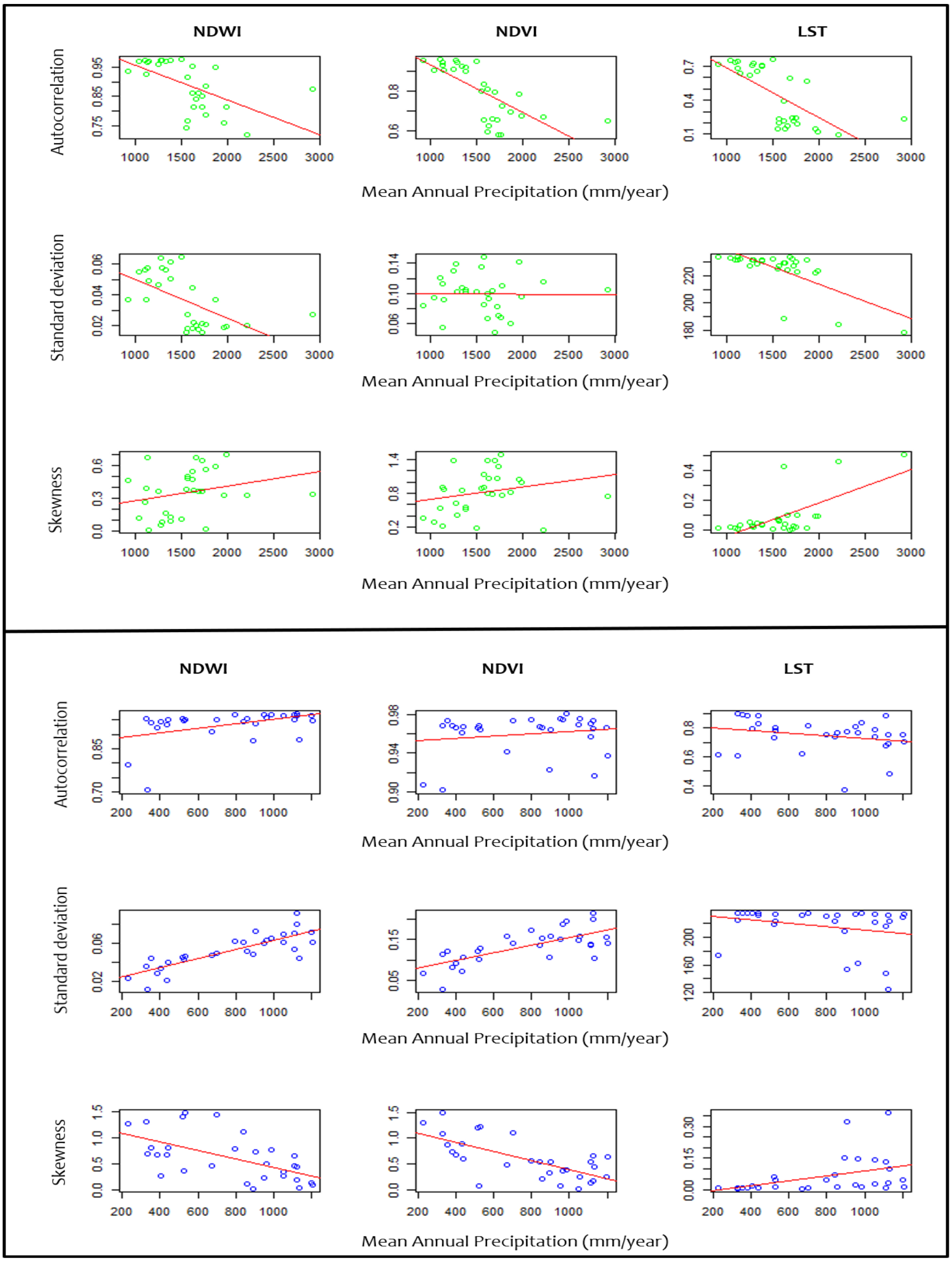

Figure A2-1. Regression analysis on relationship between mean annual precipitation and statistical stability indicators without detrending technique on high (green) and low tree cover (blue)

Appendix 2-2

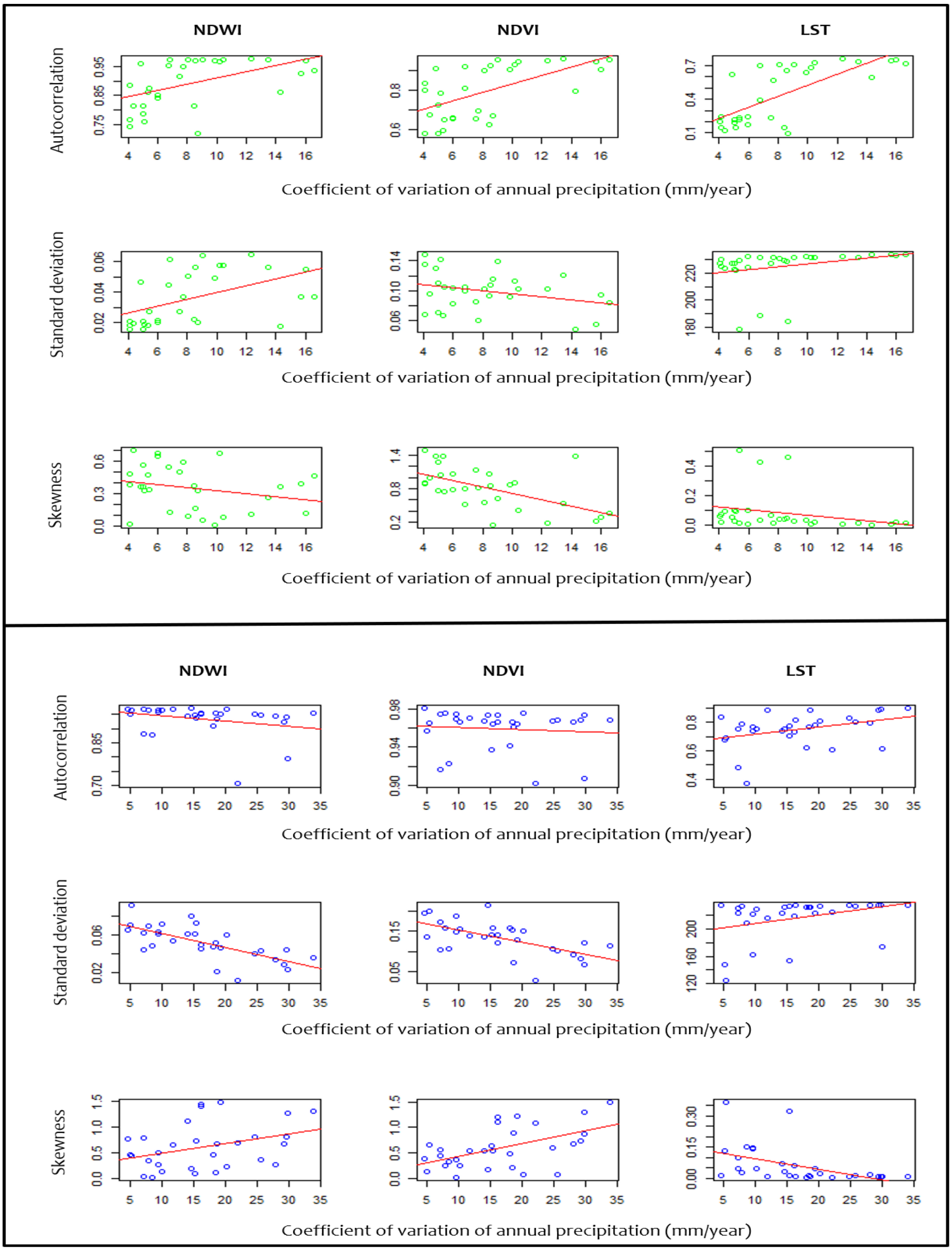

Figure A2-2. Regression analysis on relationship between coefficient of variation of annual precipitation and statistical stability indicators without detrending technique on high (green) and low tree cover (blue)

Appendix 2-3

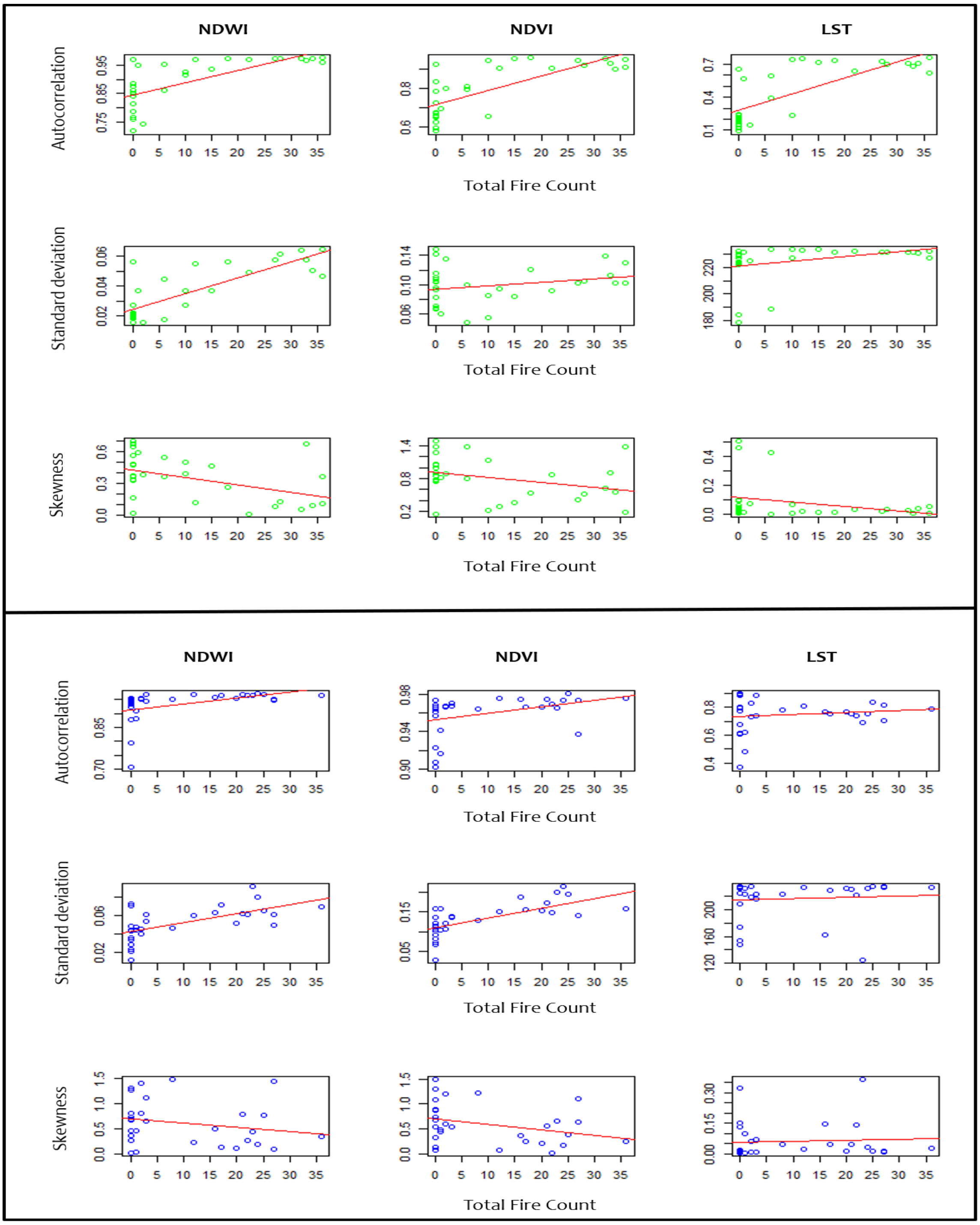

Figure A2-3. Regression analysis on relationship between total fire count and statistical stability indicators without detrending technique on high (green) and low tree cover (blue)

Appendix 2-4

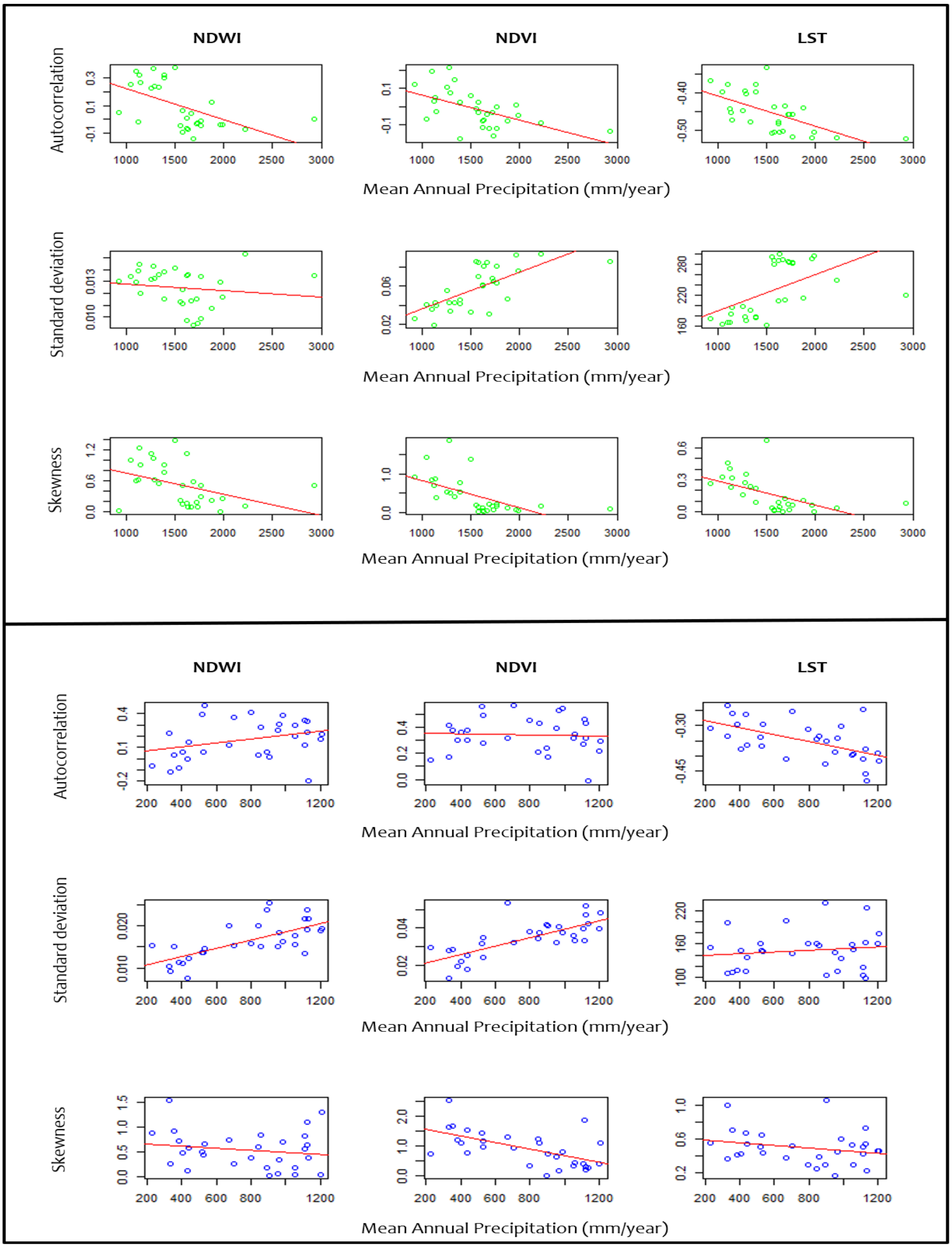

Figure A2-4. Regression analysis on relationship between mean annual precipitation and statistical stability indicators in first-differencing filter on high (green) and low tree cover (blue)

Appendix 2-5

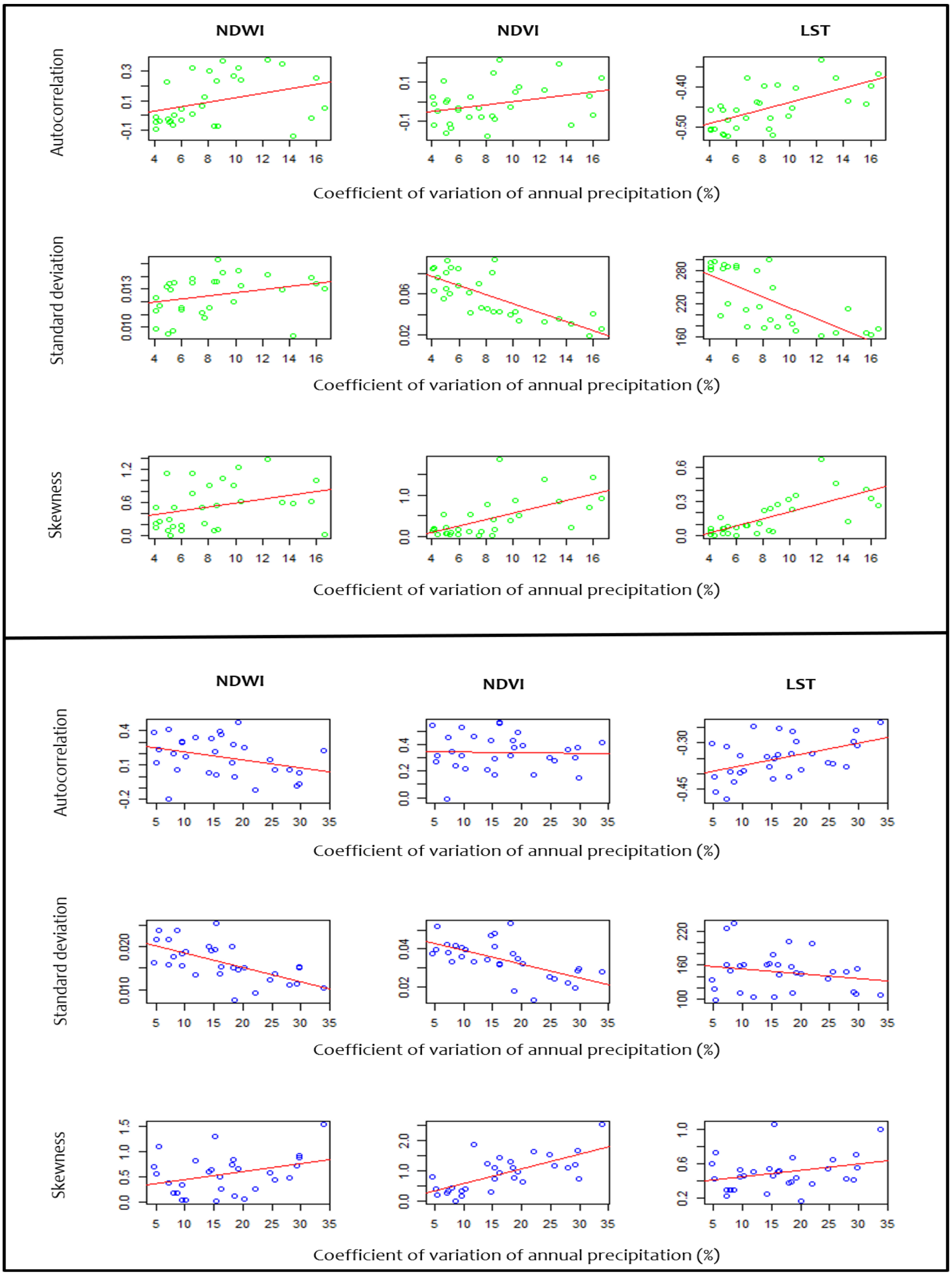

Figure A2-5. Regression analysis on relationship between coefficient of variation of annual precipitation and statistical stability indicators in first-differencing filter on high (green) and low tree cover (blue)

Appendix 2-6

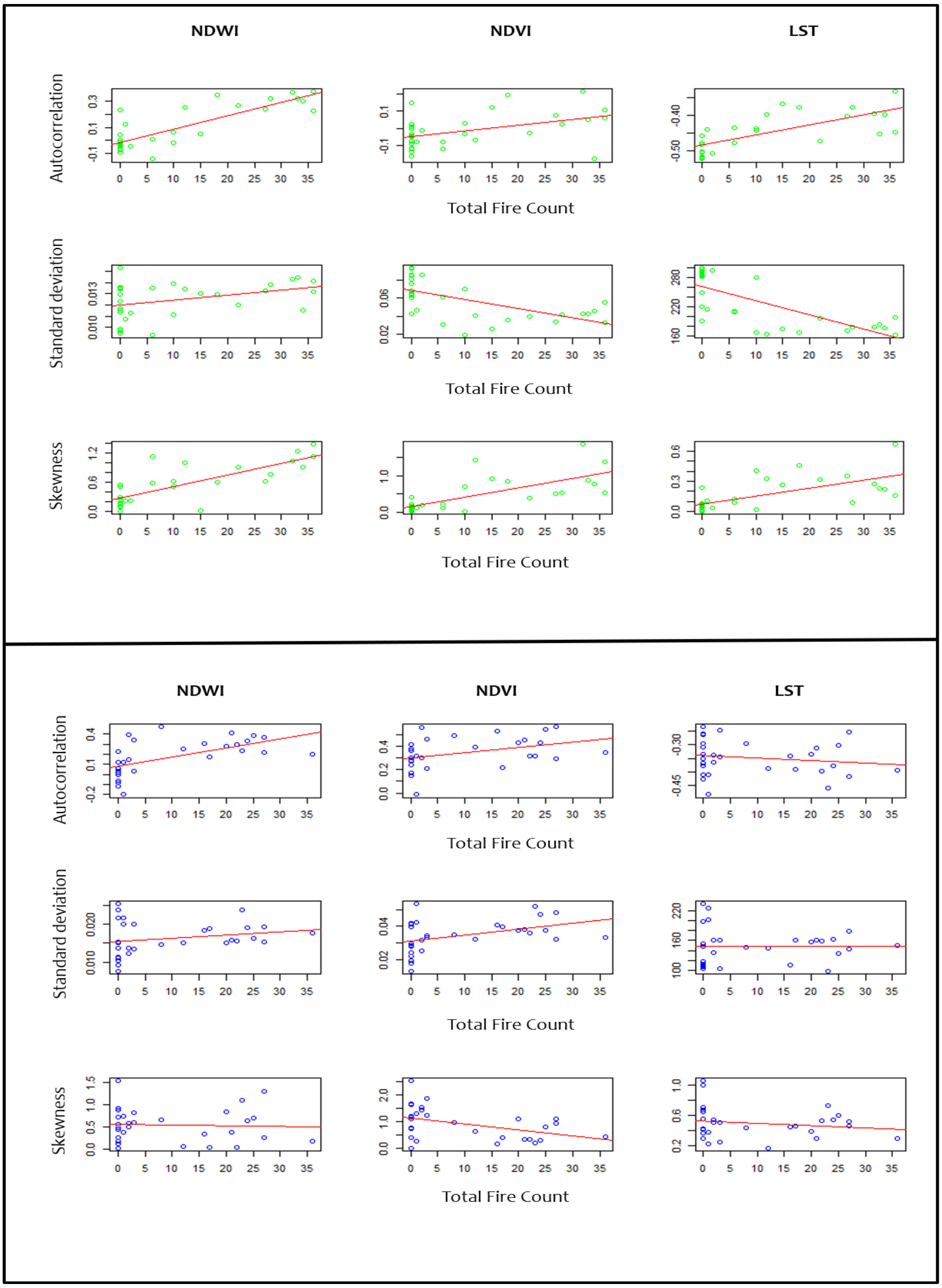

Figure A2-6. Regression analysis on relationship between total fire count and statistical stability indicators in first-differencing filter on high (green) and low tree cover (blue)

Appendix 2-7

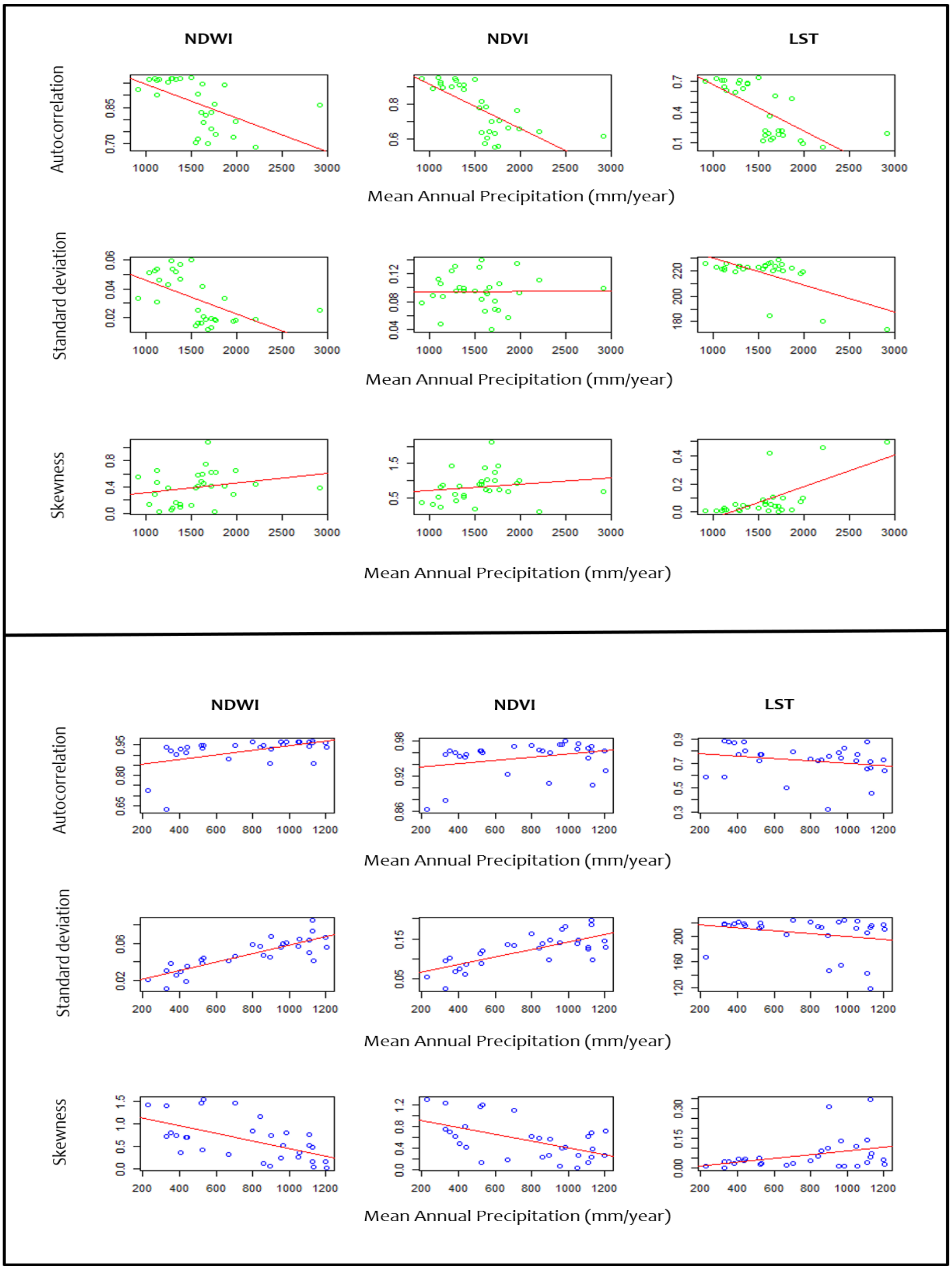

Figure A2-7. Regression analysis on relationship between mean annual precipitation and statistical stability indicators in gaussian filtering on high (green) and low tree cover (blue)

Appendix 2-8

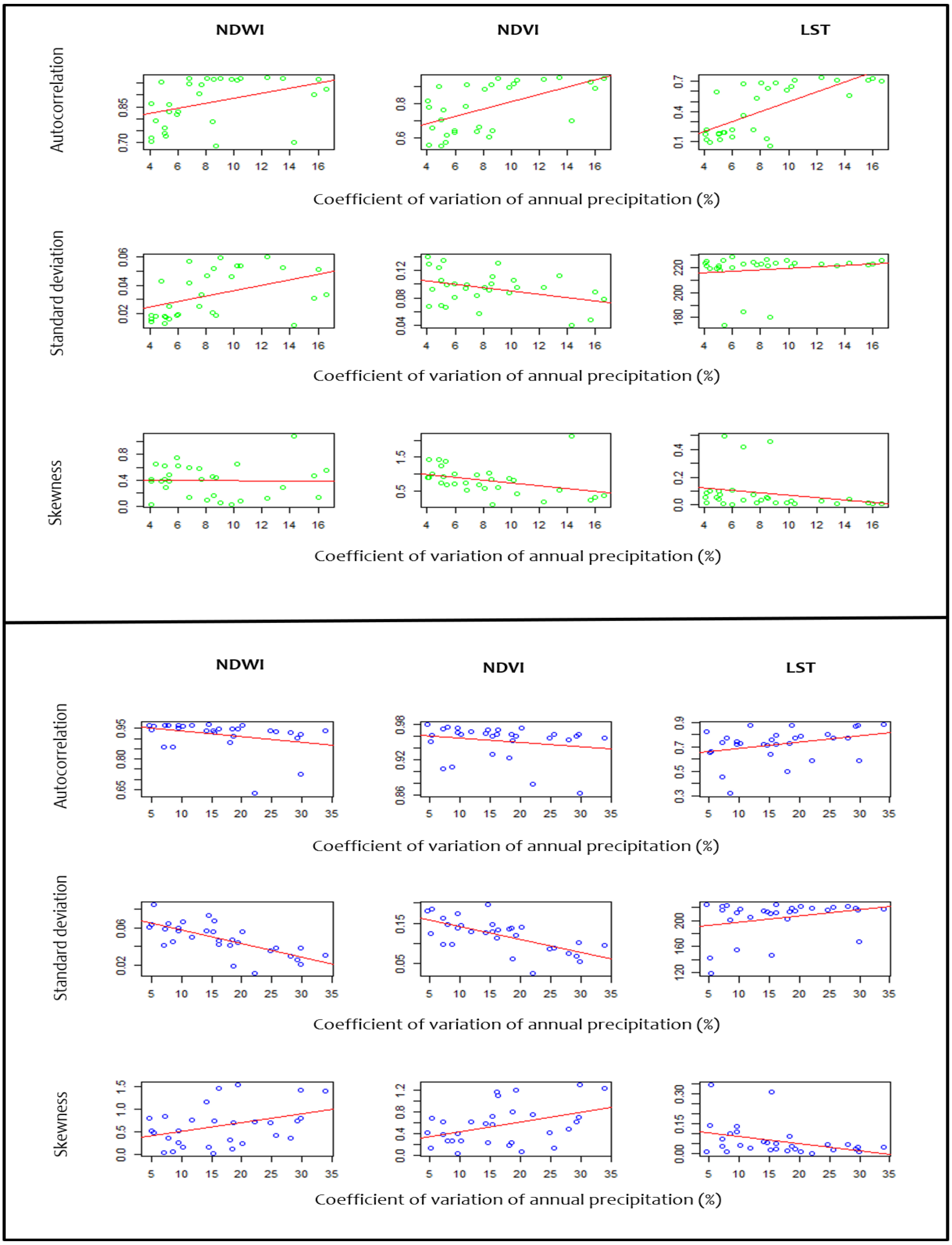

Figure A2-8. Regression analysis on relationship between coefficient of variation of annual precipitation and statistical stability indicators in gaussian filtering on high (green) and low tree cover (blue)

Appendix 2-9

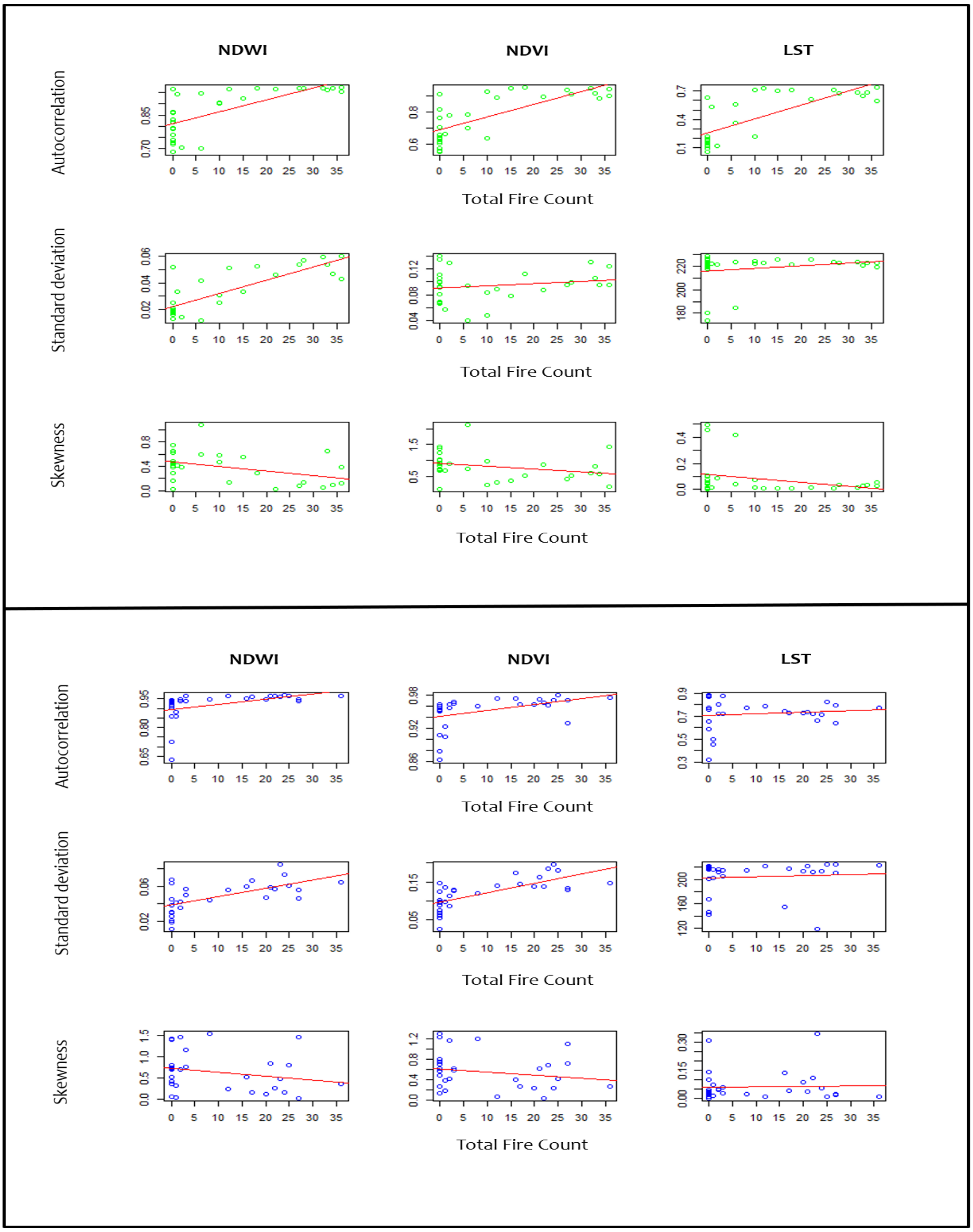

Figure A2-9. Regression analysis on relationship between total fire count and statistical stability indicators in gaussian filtering on high (green) and low tree cover (blue)

Appendix 2-10

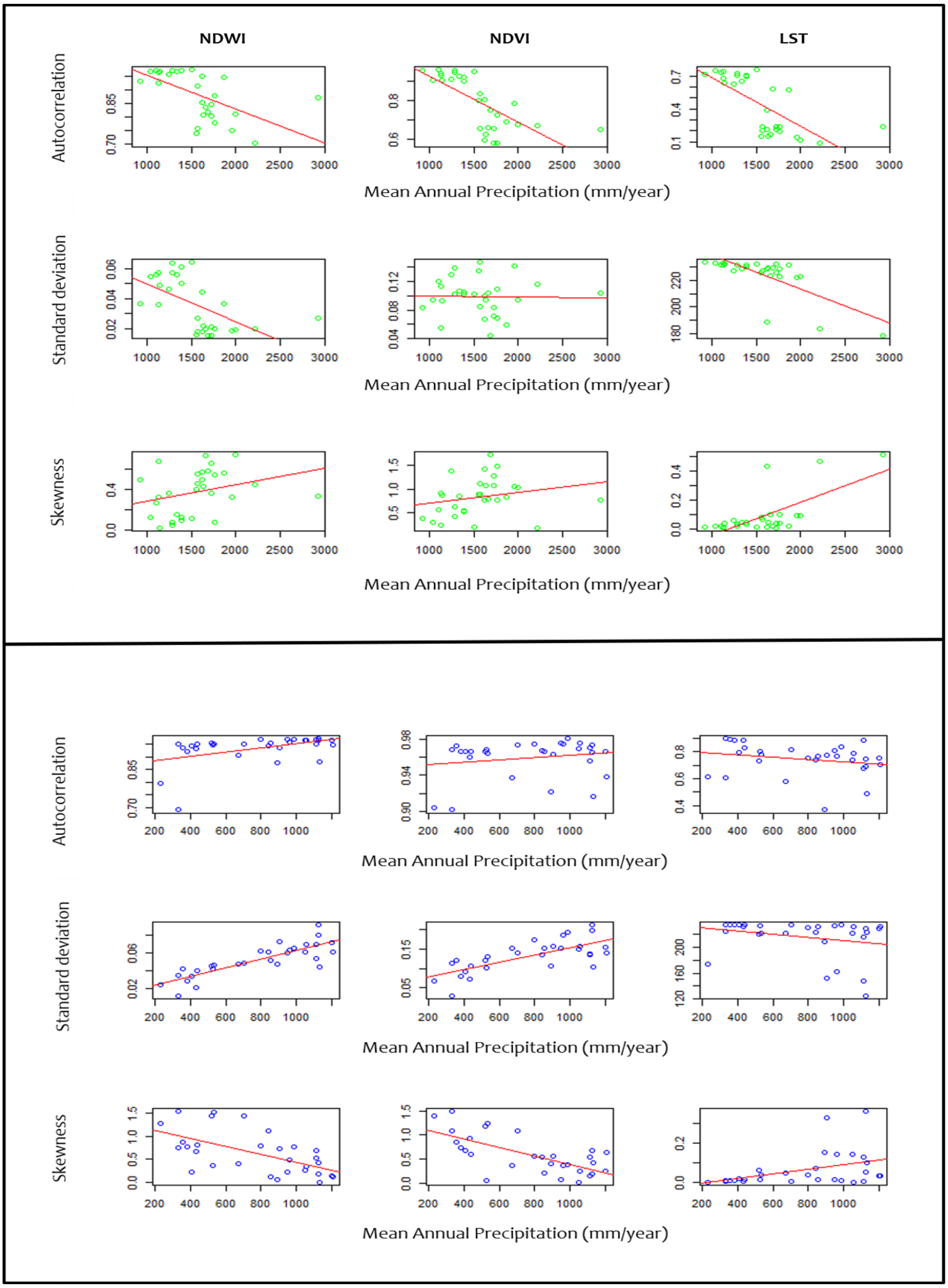

Figure A2-10. Regression analysis on relationship between mean annual precipitation and statistical stability indicators in linear detrending on high (green) and low tree cover (blue)

Appendix 2-11

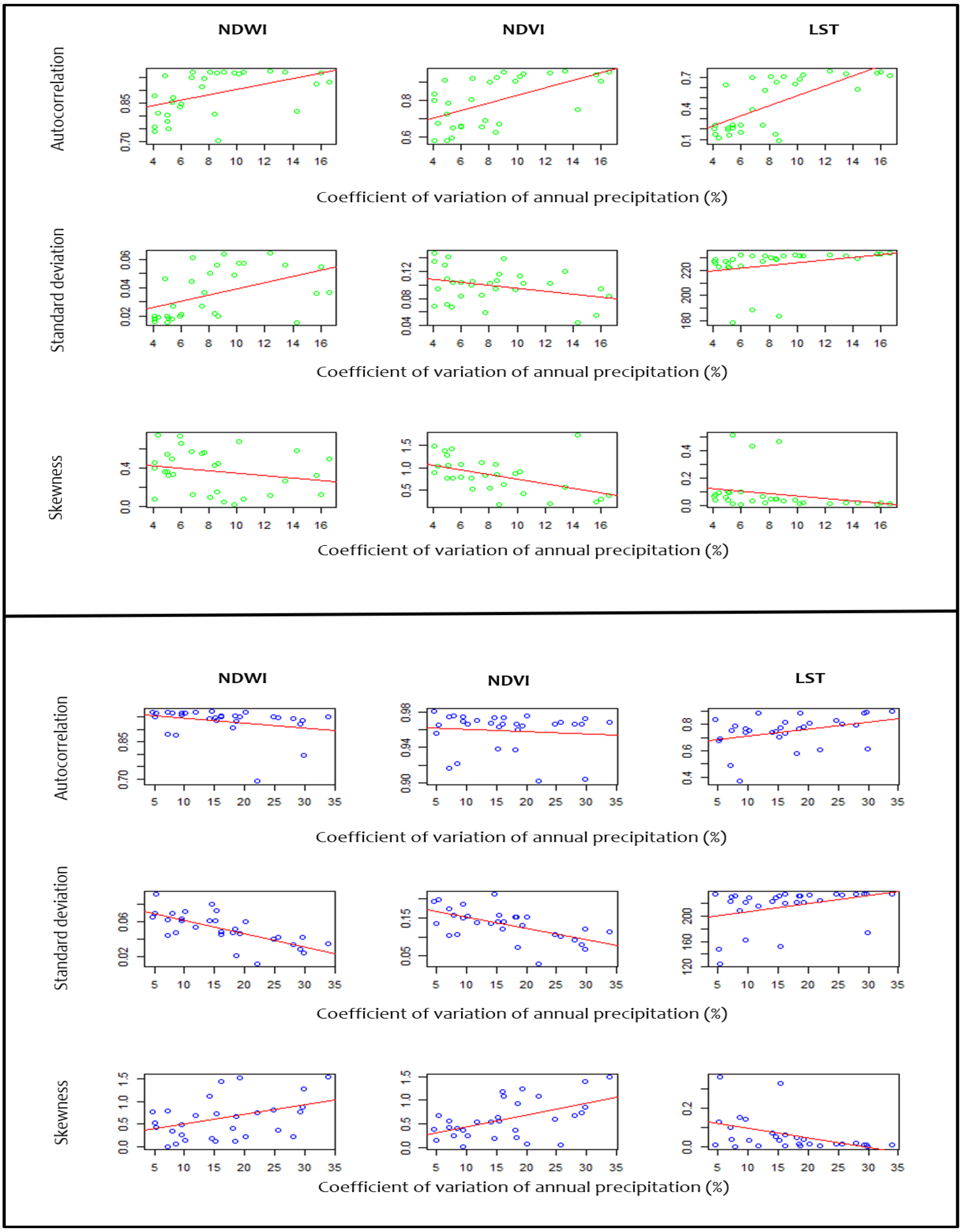

Figure A2-11. Regression analysis on relationship between coefficient of variation of annual precipitation and statistical stability indicators in linear detrending on high (green) and low tree cover (blue)

Appendix 2-12

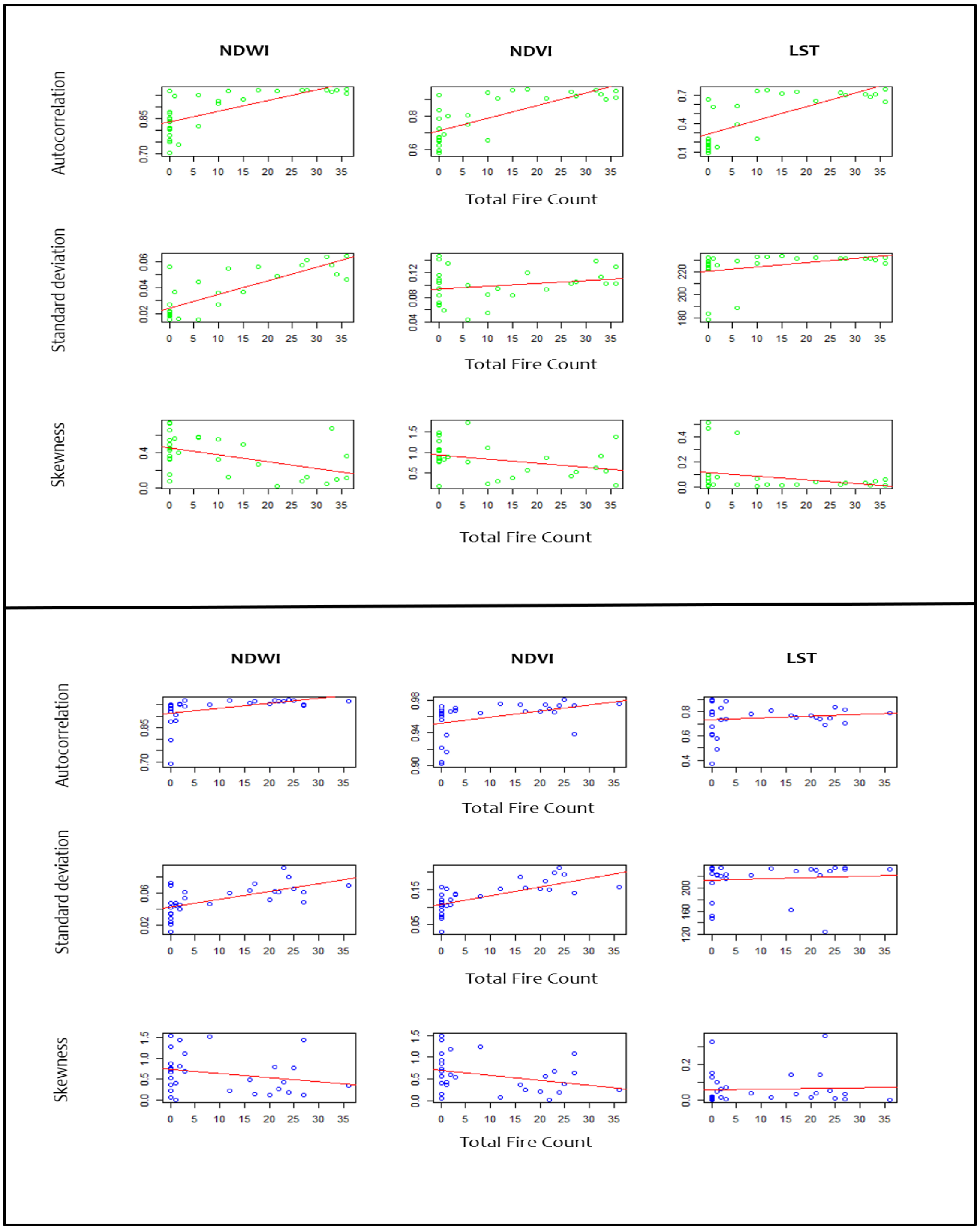

Figure A2-12. Regression analysis on relationship between total fire count and statistical stability indicators in linear detrending on high (green) and low tree cover (blue)

Appendix 3-1

Table A3-1. R-squared and trend significance between tree cover and environmental drivers without detrending technique

Environmental driver	Tree cover (%)	Statistical stability indicators	NDWI	NDVI	LST
Mean annual precipitation	High	Autocorrelation	0.34***	0.5***	0.49***
		Standard deviation	0.34***	0.00	0.5***
		Skewness	0.07	0.05	0.45***
	Low	Autocorrelation	0.19*	0.03	0.05
		Standard deviation	0.69***	0.49***	0.06
		Skewness	0.34***	0.47***	0.17*
Coefficient of variation of annual precipitation	High	Autocorrelation	0.25**	0.35***	0.52***
		Standard deviation	0.02	0.10	0.09
		Skewness	0.07	0.33***	0.07
	Low	Autocorrelation	0.07	0.01	0.13
		Standard deviation	0.48***	0.35***	0.12
		Skewness	0.13	0.28**	0.23**
Total fire count	High	Autocorrelation	0.51***	0.55***	0.58***
		Standard deviation	0.67***	0.06	0.11
		Skewness	0.2*	0.11	0.09
	Low	Autocorrelation	0.18*	0.14*	0.02
		Standard deviation	0.37***	0.45***	0.01
		Skewness	0.05	0.10	0.00

Appendix 3-2

Table A3-2. R-squared and trend significance between tree cover and environmental drivers in first-differencing filter

Environmental driver	Tree cover (%)	Statistical stability indicators	NDWI	NDVI	LST
Mean annual precipitation	High	Autocorrelation	0.3**	0.31**	0.39***
		Standard deviation	0.02	0.5***	0.29**
		Skewness	0.17*	0.35***	0.31**
	Low	Autocorrelation	0.09	0.00	0.31**
		Standard deviation	0.47***	0.54***	0.02
		Skewness	0.03	0.34***	0.06
Coefficient of variation of annual precipitation	High	Autocorrelation	0.12	0.10	0.41***
		Standard deviation	0.09	0.58***	0.52***
		Skewness	0.10	0.38***	0.52***
	Low	Autocorrelation	0.11	0.00	0.23**
		Standard deviation	0.39***	0.39***	0.04
		Skewness	0.12	0.47***	0.09
Total fire count	High	Autocorrelation	0.7***	0.2*	0.52***
		Standard deviation	0.15*	0.38***	0.54***
		Skewness	0.62***	0.51***	0.43***
	Low	Autocorrelation	0.36***	0.15*	0.03
		Standard deviation	0.05	0.19*	0.00
		Skewness	0.00	0.18*	0.03

Appendix 3-3

Table A3-3. R-squared and trend significance between tree cover and environmental drivers in gaussian filtering

Environmental driver	Tree cover (%)	Statistical stability indicators	NDWI	NDVI	LST
Mean annual precipitation	High	Autocorrelation	0.3**	0.53***	0.51***
		Standard deviation	0.32**	0.00	0.41***
		Skewness	0.06	0.03	0.47***
	Low	Autocorrelation	0.22**	0.09	0.05
		Standard deviation	0.7***	0.55***	0.06
		Skewness	0.34***	0.3**	0.13
Coefficient of variation of annual precipitation	High	Autocorrelation	0.16*	0.32**	0.52***
		Standard deviation	0.09	0.13*	0.03
		Skewness	0.00	0.14*	0.06
	Low	Autocorrelation	0.10	0.05	0.12
		Standard deviation	0.52***	0.42***	0.09
		Skewness	0.13	0.16*	0.14*
Total fire count	High	Autocorrelation	0.49***	0.57***	0.59***
		Standard deviation	0.66***	0.04	0.05
		Skewness	0.18*	0.07	0.10
	Low	Autocorrelation	0.19*	0.19*	0.01
		Standard deviation	0.4***	0.49***	0.01
		Skewness	0.05	0.04	0.00

Appendix 4-1

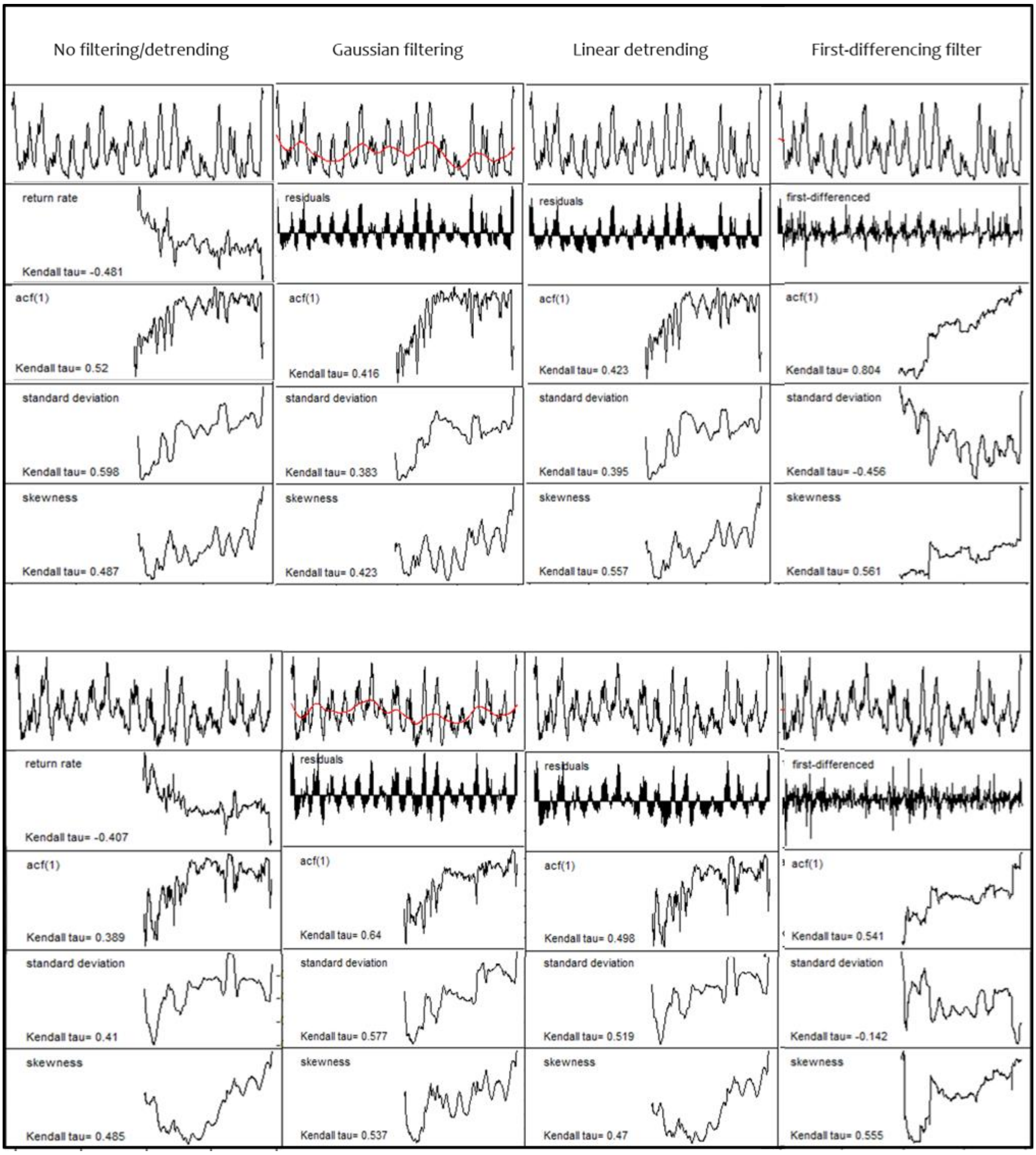

Figure A4-1. Time series profiles of NDVI (upper) and NDWI (lower) on an area with low tree cover percentage located at 27^0 S and 24^0 E in different detrending methods, showing increasing trends on statistical measurements, except on standard deviation in first-differencing filtering method

Appendix 4-2

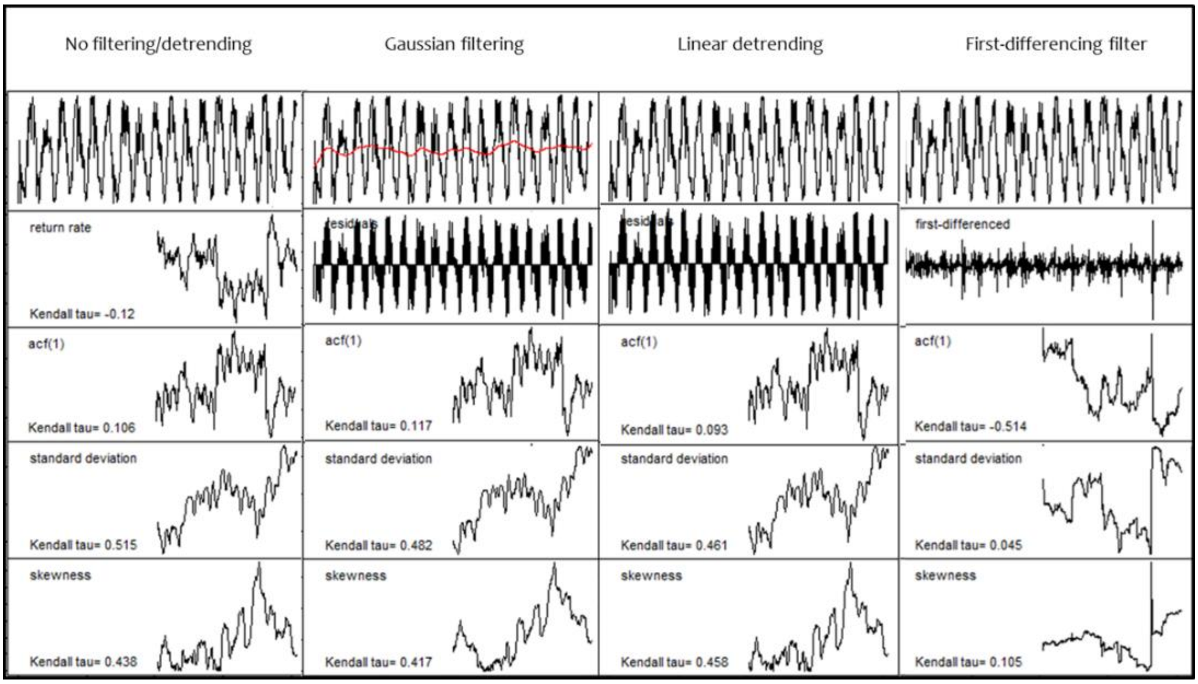

Figure A4-2. Time series profiles of LST on an area with low tree cover percentage located at 27^0 S and 24^0 E in different detrending methods, showing increasing trends on statistical measurements, except on standard deviation in first-differencing filtering method

Appendix 5

Programming Information

a. Data extraction on mean annual precipitation from CHIRPS data with tree cover extent in Google Earth Engine

```
// Sub-Saharan boundary
var sample = (table);
Map.addLayer({eeObject : sample,
              name: "sample"});

// CHIRPS in 2000-2010
var collection_precipitation = ee.ImageCollection('UCSB-CHG/CHIRPS/PENTAD')
    .filterDate('2000-01-01', '2010-12-31');
Map.addLayer(collection_precipitation);

// Reduce collection to image (average)
var total_precipitation = collection_precipitation.sum();
var mean_precipitation = total_precipitation.divide(11);

// Clip with shapefiles in Sub Saharan and convert the image to vector
var mean_precipitationVectors = mean_precipitation.reduceRegions({
  collection: sample,
  crs: mean_precipitation.projection(),
  scale: 1000,
  reducer: ee.Reducer.mean()
});

// Export the FeatureCollection.
Export.table.toDrive({
  collection: mean_precipitationVectors,
  description: 'tree-mean_precipitation',
  folder: 'Precipitation',
  fileNamePrefix: 'tree-mean_precipitation',
  fileFormat: 'CSV',
  selectors : 'polyname,mean,TC_percent'
  });
```

table = the shapefile of areas covered by trees (TC and TCM areas)

b. Data extraction on standard deviation of annual precipitation from CHIRPS data with tree cover extent in Google Earth Engine, to calculate coefficient of variation of annual precipitation

```
// Sub-Saharan boundary
var sample = (table);
Map.addLayer({eeObject : sample,
              name: "sample"});

// Annual collection between 2000-2010
var collection1 = ee.ImageCollection('UCSB-CHG/CHIRPS/PENTAD')
    .filterDate('2000-01-01', '2000-12-31');
var collection2 = ee.ImageCollection('UCSB-CHG/CHIRPS/PENTAD')
    .filterDate('2001-01-01', '2001-12-31');
var collection3 = ee.ImageCollection('UCSB-CHG/CHIRPS/PENTAD')
    .filterDate('2002-01-01', '2002-12-31');
var collection4 = ee.ImageCollection('UCSB-CHG/CHIRPS/PENTAD')
    .filterDate('2003-01-01', '2003-12-31');
var collection5 = ee.ImageCollection('UCSB-CHG/CHIRPS/PENTAD')
    .filterDate('2004-01-01', '2004-12-31');
var collection6 = ee.ImageCollection('UCSB-CHG/CHIRPS/PENTAD')
    .filterDate('2005-01-01', '2005-12-31');
var collection7 = ee.ImageCollection('UCSB-CHG/CHIRPS/PENTAD')
    .filterDate('2006-01-01', '2006-12-31');
var collection8 = ee.ImageCollection('UCSB-CHG/CHIRPS/PENTAD')
    .filterDate('2007-01-01', '2007-12-31');
var collection9 = ee.ImageCollection('UCSB-CHG/CHIRPS/PENTAD')
    .filterDate('2008-01-01', '2008-12-31');
var collection10 = ee.ImageCollection('UCSB-CHG/CHIRPS/PENTAD')
    .filterDate('2009-01-01', '2009-12-31');
var collection11 = ee.ImageCollection('UCSB-CHG/CHIRPS/PENTAD')
    .filterDate('2010-01-01', '2010-12-31');


// Yearly image collection to image
var image1 = collection1.sum();
var image2 = collection2.sum();
var image3 = collection3.sum();
var image4 = collection4.sum();
var image5 = collection5.sum();
var image6 = collection6.sum();
var image7 = collection7.sum();
var image8 = collection8.sum();
var image9 = collection9.sum();
var image10 = collection10.sum();
var image11 = collection11.sum();

// CHIRPS in 2000-2010
var collection_precipitation = ee.ImageCollection('UCSB-CHG/CHIRPS/PENTAD')
    .filterDate('2000-01-01', '2010-12-31');
//Map.addLayer(collection_precipitation);

// Reduce collection to image (average)
var total_precipitation = collection_precipitation.sum();
var mean_precipitation = total_precipitation.divide(11);


// Subtraction to the mean
var subtract1 = image1.subtract(mean_precipitation);
var subtract2 = image2.subtract(mean_precipitation);
var subtract3 = image3.subtract(mean_precipitation);
var subtract4 = image4.subtract(mean_precipitation);
var subtract5 = image5.subtract(mean_precipitation);
```

table = the shapefile of areas covered by trees (TC and TCM areas)

```
var subtract6 = image6.subtract(mean_precipitation);
var subtract7 = image7.subtract(mean_precipitation);
var subtract8 = image8.subtract(mean_precipitation);
var subtract9 = image9.subtract(mean_precipitation);
var subtract10 = image10.subtract(mean_precipitation);
var subtract11 = image11.subtract(mean_precipitation);

// Squared subtraction
var square1 = subtract1.multiply(subtract1);
var square2 = subtract2.multiply(subtract2);
var square3 = subtract3.multiply(subtract3);
var square4 = subtract4.multiply(subtract4);
var square5 = subtract5.multiply(subtract5);
var square6 = subtract6.multiply(subtract6);
var square7 = subtract7.multiply(subtract7);
var square8 = subtract8.multiply(subtract8);
var square9 = subtract9.multiply(subtract9);
var square10 = subtract10.multiply(subtract10);
var square11 = subtract11.multiply(subtract11);

// Total and mean difference
var total_difference = square1.add(square2).add(square3).add(square4).add(square5)
                        .add(square6).add(square7).add(square8).add(square9)
                        .add(square10).add(square11);
var mean_difference = total_difference.divide(11);

// Standard deviation
var sd_precipitation = mean_difference.sqrt();

// Convert the image to vector
var sd_precipitationVectors = sd_precipitation.reduceRegions({
  collection: sample,
  crs: sd_precipitation.projection(),
  scale: 1000,
  reducer: ee.Reducer.mean()
});

// Export the FeatureCollection.
Export.table.toDrive({
  collection: sd_precipitationVectors,
  description: 'tree-sd_precipitation',
  folder: 'Precipitation',
  fileNamePrefix: 'tree-sd_precipitation',
  fileFormat: 'CSV',
  selectors : 'polyname,mean,TC_percent'
  });

```

c. Data extraction on total fire count from MODIS MCD45A1 burned area product with tree cover extent in Google Earth Engine

```
// Sub-Saharan boundary
var sample = (table);
Map.addLayer({eeObject : sample,
              name: "sample"});

// Fire in Sub-Saharan Africa (2010-2010)
var collection_fire = ee.ImageCollection('MODIS/051/MCD45A1')
    .filterDate('2000-01-01', '2010-12-31');
Map.addLayer(collection_fire);

// Reduce collection to image (total)
var total_fire = collection_fire.sum();

// Convert the image to vector
var fireVectors = total_fire.reduceRegions({
  collection: sample,
  crs: total_fire.projection(),
  scale: 1000,
  reducer: ee.Reducer.mean()
});

// Export the FeatureCollection.
Export.table.toDrive({
  collection: fireVectors,
  fileNamePrefix: 'tree-fire',
  fileFormat: 'CSV',
  selectors : 'polyname,direction'
});

```

table = the shapefile of areas covered by trees (TC and TCM areas)

d. Extraction of generic early warning signals and detrending techniques in R-environment

```r
## SCRIPT TO DETREND AND TIME SERIES AND EXTRACT EARLY WARNING SIGNALS) FROM SATELLITE TIME SERIES
## WRITTEN BY THOMAS GROEN (T.A.GROEN@UTWENTE.NL) AND EUFRASIA BIANCA DIATMIKO (e.b.diatmiko@student.utwente.nl)

setwd("C:\\Users\\inka_diatmiko\\Documents\\ArcGIS\\Thesis\\2nd objective\\Detrending")

##load the early warnings signal package that has the right function
###make sure these are installed before calling them here.
require(earlywarnings) ##needed for detrending and calculations of indicators
require(gdata) ## needed to read in excel files
require(zoo) ## needed for filling gaps in timeseries
library(earlywarnings)
library(gdata)
library(zoo)


##set local settings to make sure the date conversion works as planned
Sys.setlocale("LC_TIME", locale = "us")

## SCRIPT WHEN HAVING ALL SERIES IN ONE FILE
result<-NULL
##open the file
d<-read.csv("NDVI_highTC.csv")

# ##convert the date from text to numerical values
# d$date<-as.numeric(as.Date(d[,1],'%Y-%m-%d'))

for(i in (2:(length(d$Time))))#i=2
{
  ##select the right columns
  temp<-d[,i]
  ##fill the gaps by linear interpolation
  temp<-na.approx(temp)
  r<-generic_ews(temp,winsize=99,detrending="linear")
  ##save the indicators in the summary table
  result<-rbind(result,
                data.frame(name=names(d)[i],##file name of location and biomestate indicator
                           acf1=mean(r$acf1),##autocorrelation-at-lag-1
                           sd=mean(r$sd),## standard deviation
                           cv=mean(r$cv),## coefficient of variation
                           sk=mean(r$sk)))## Skewness
}

##Save results of statistical stability indicators in CSV table
write.csv(result, file = "NDVI_highTC_linear.csv")

##More information on generic early warning signals
?earlywarnings

```